Geophysical Geodesy
Tuesday September 27, 2011

- Field trip logistics, head count
- Kreemer and Hammond, 2007
- Class Thursday 9AM

- Continuum Tensor Strain Rate Maps
- Block Models

- New Reading:

1) in preparation for field trip: Smith et al., 2004
2) Chapter 2 of Earthquake and Volcano Deformation

- Discussion leader for Smith et al., 2004

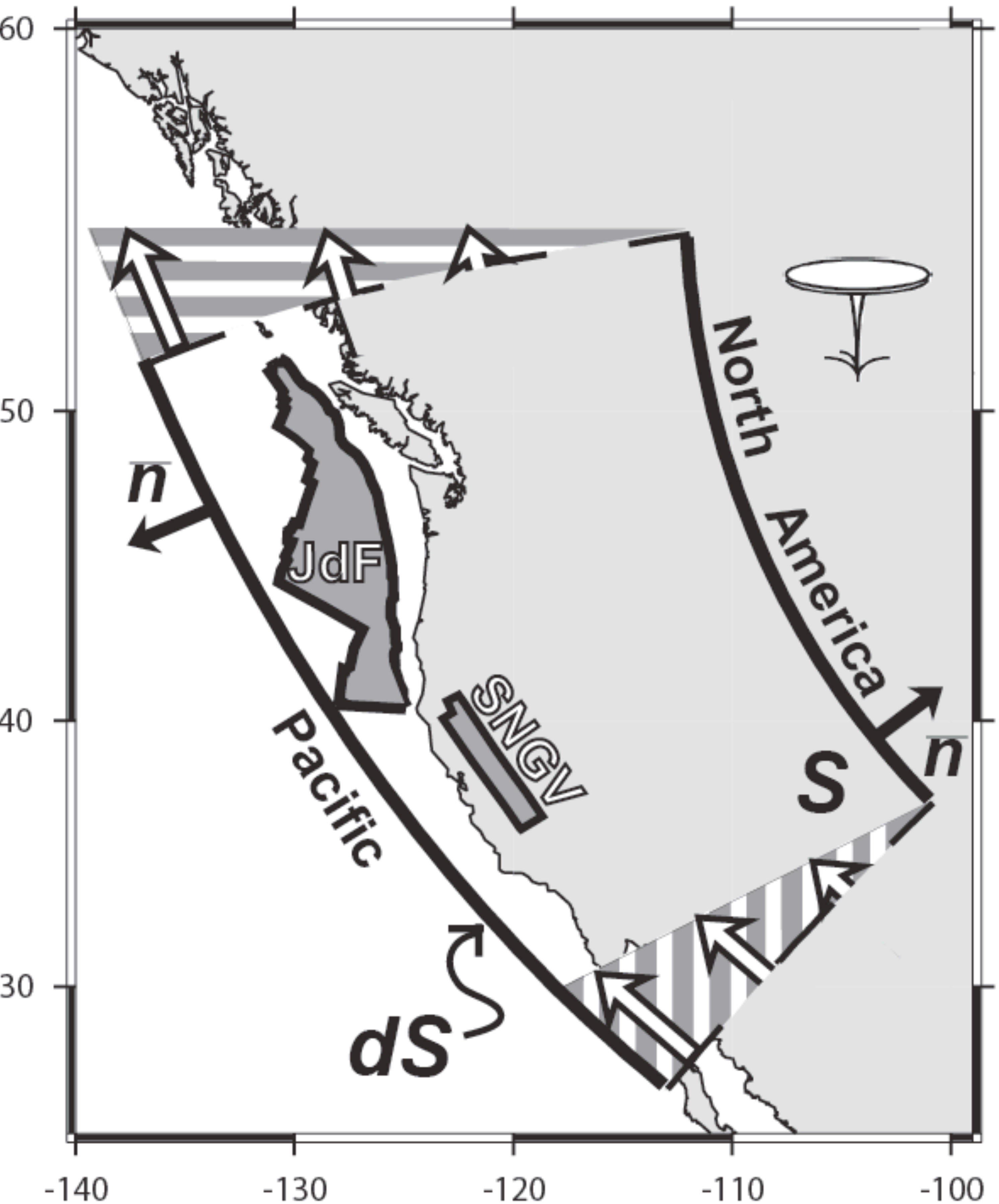

Gauss' Divergence Theorem:

$$\oint_{\partial S} (\overline{v} \cdot \overline{n})\, dl = R^2 \iint_S (\nabla \cdot \overline{v}) \cos\theta\, d\theta\, d\varphi$$

$$\iint_S \left(\dot{\varepsilon}_{\theta\theta} + \dot{\varepsilon}_{\varphi\varphi}\right) \cos\theta\, d\theta\, d\varphi = \dot{A} / R^2$$

Great Circle

Small Circle

Kreemer and Hammond, 2007

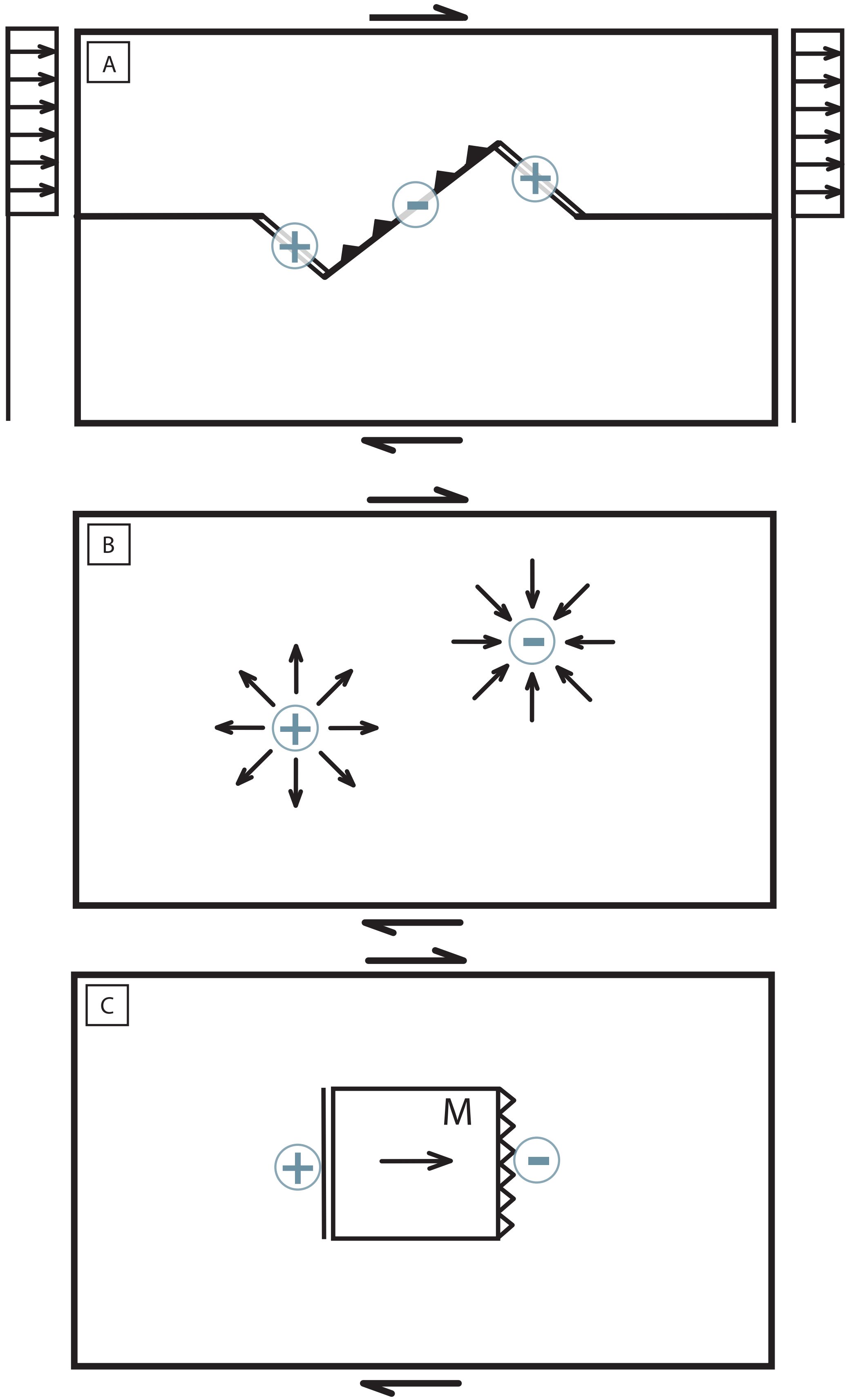

Gauss' Divergence Theorem:

$$\oint_{\partial S} (\overline{v} \cdot \overline{n})\, dl = R^2 \iint_S (\nabla \cdot \overline{v}) \cos\theta\, d\theta\, d\varphi$$

$$\iint_S \left(\dot{\varepsilon}_{\theta\theta} + \dot{\varepsilon}_{\varphi\varphi}\right) \cos\theta\, d\theta\, d\varphi = \dot{A} / R^2$$

Simple Examples: Two plate boundaries and a shear zone

Kreemer and Hammond, 2007

Separate the tensor strain rate into dilatation and shear components

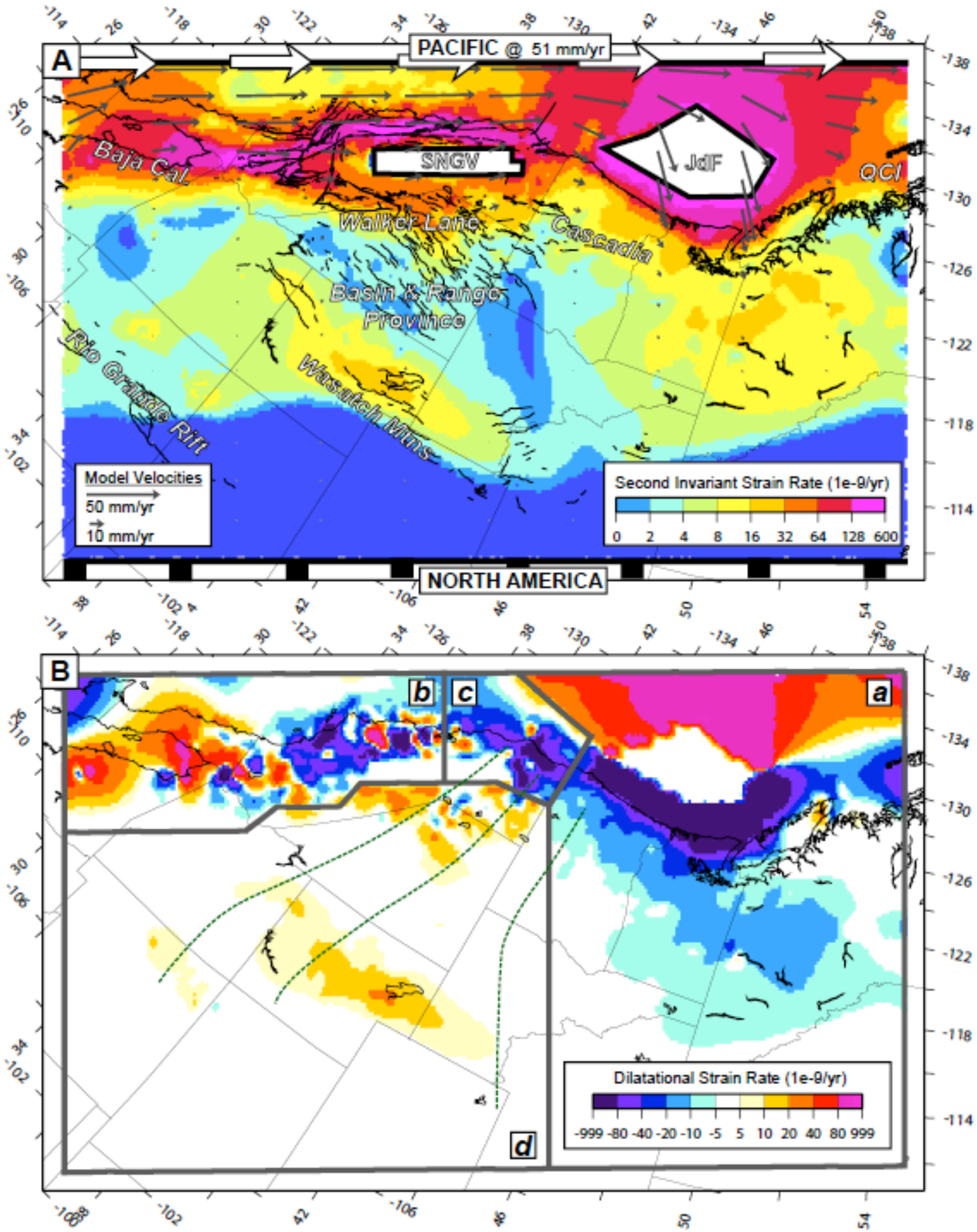

TABLE 1. AREAL CHANGE AND VELOCITY FLUX

Region	$\dot{A}$ (m^2 yr^{-1})	$\oint \bar{v} \cdot \bar{n}$ (mm yr^{-1})
a. Cascadia–Juan de Fuca	221 ± 287	0.1 ± 0.2
areal reduction	–32,391	–19.2
areal growth	32,612	19.3
b. San Andreas fault system	–236 ± 172	–0.1 ± 0.1
areal reduction	–8355	–4.9
areal growth	8120	4.8
c. N. California–S. Cascadia	–5021 ± 101	–3.0 ± 0.1
areal reduction	–5391	–3.2
areal growth	369	0.2
d. Basin and Range province	5193 ± 125	3.1 ± 0.1
areal reduction	–227	–0.1
areal growth	5391	3.2
TOTAL	157 ± 372	0.1 ± 0.2
areal reduction	–46,364	–27.4
areal growth	46,521	27.5

$\dot{A}$ is the integrated areal change (positive is areal growth), which is proportional to velocity flux, $\oint \bar{v} \cdot \bar{n}$. Uncertainties are one standard deviation.

PA-NA Dilatation

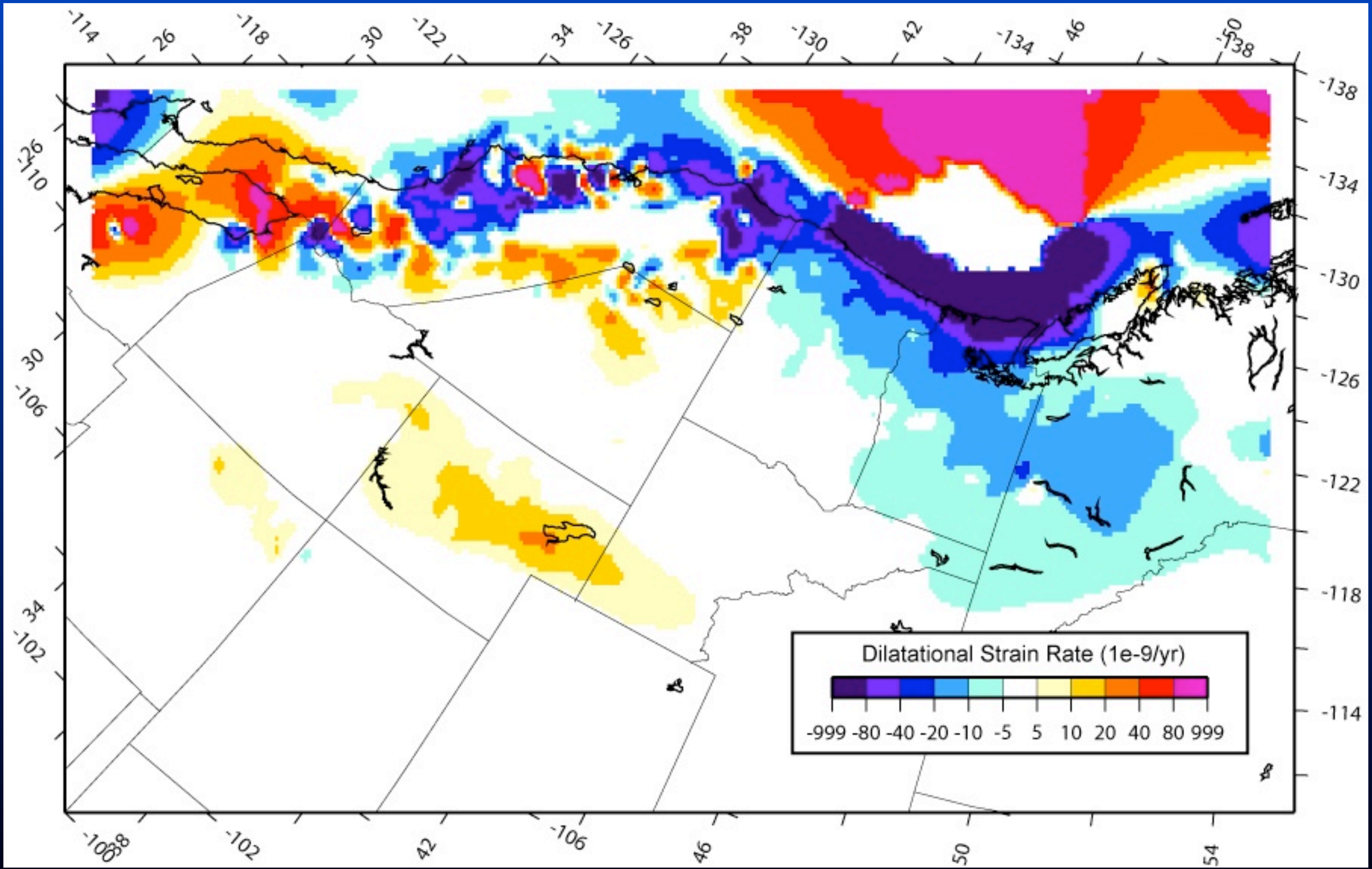

PA–NA Dilatation

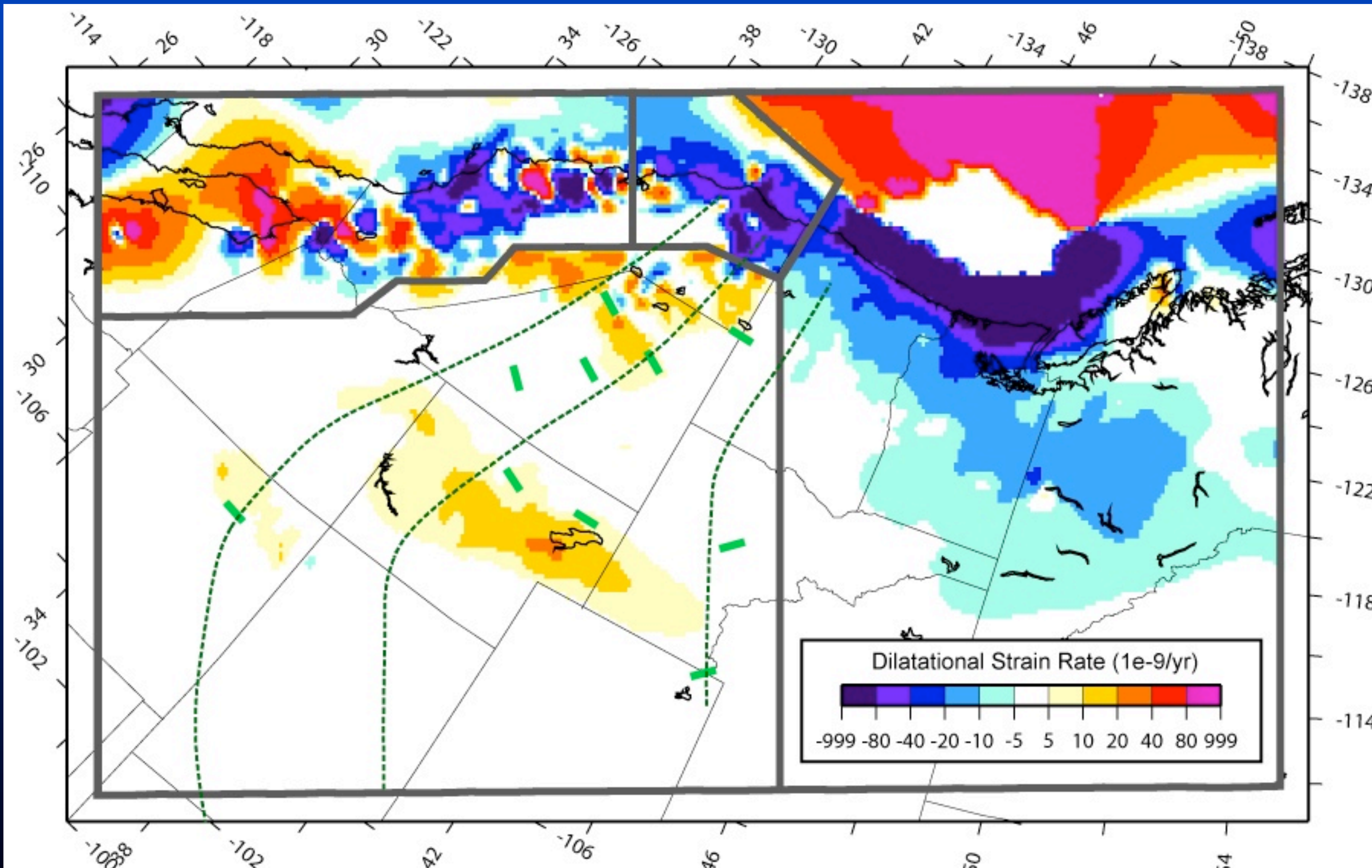

Least compressive stress trajectories and indicators from Humphreys and Coblentz, 2007
Based on World Stress Map data and modeling of forces on North American plate.

Stress Directions

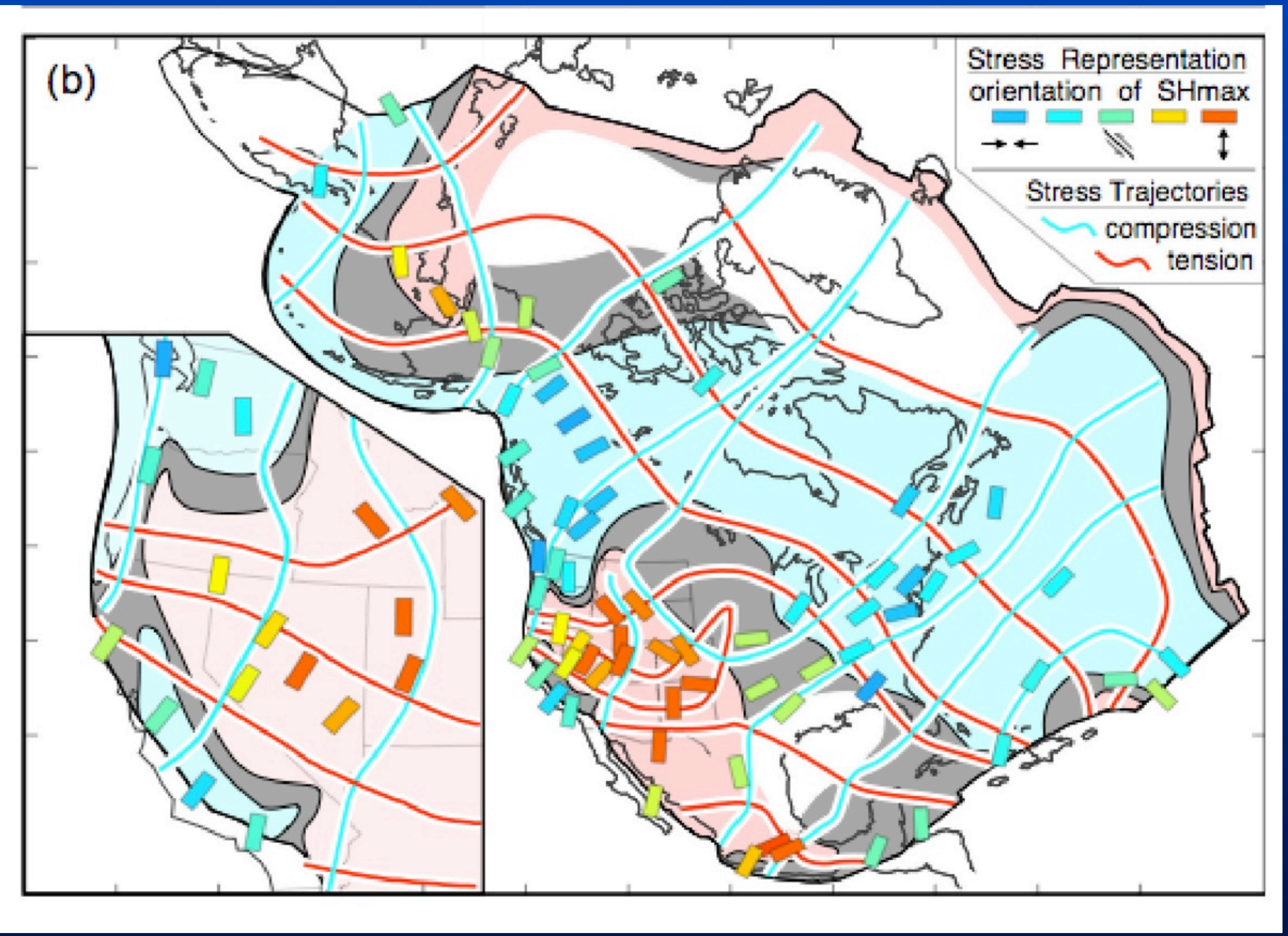

Humphreys and Coblentz, '07

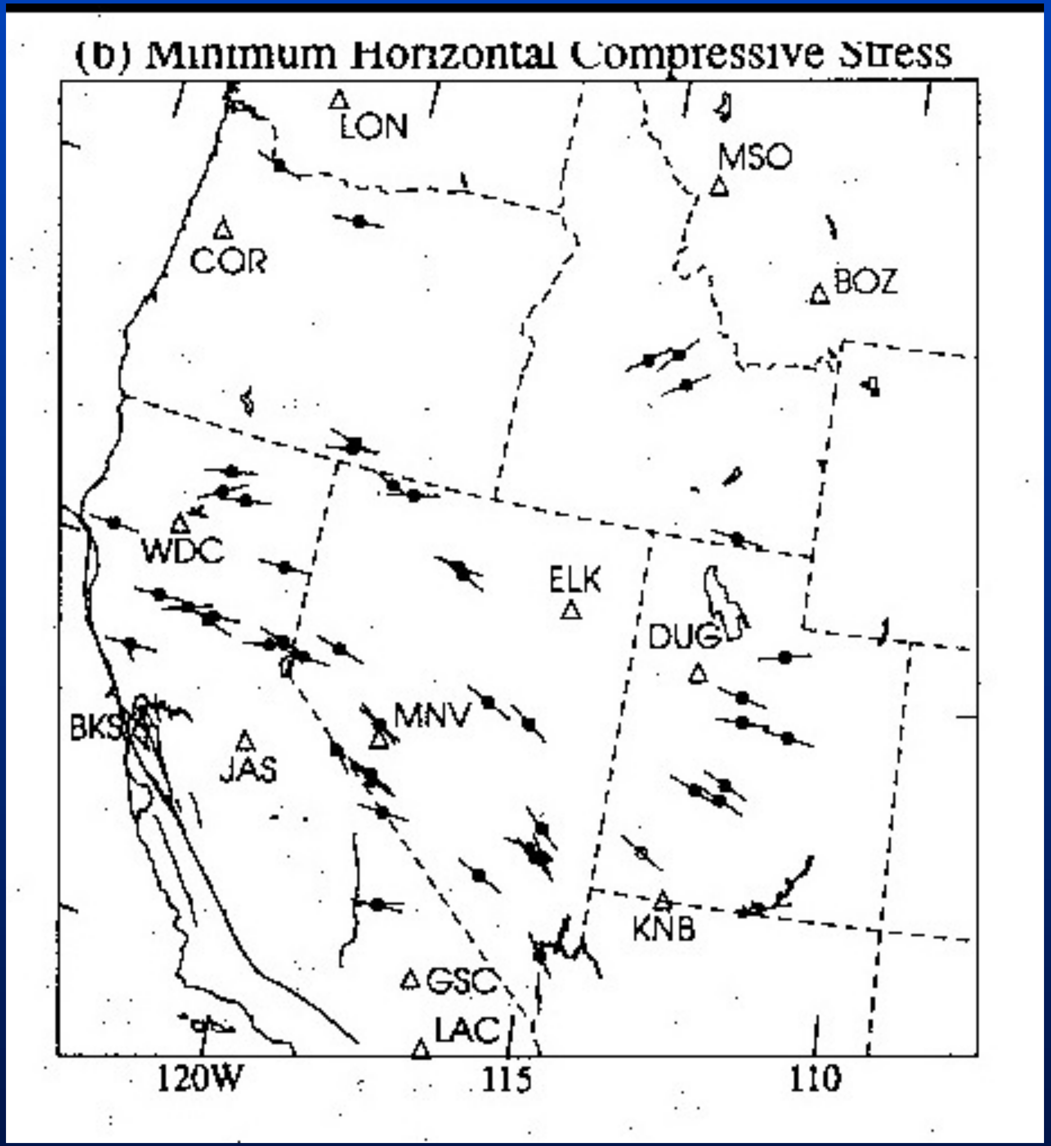

Patton and Zandt, '91

2009 Model

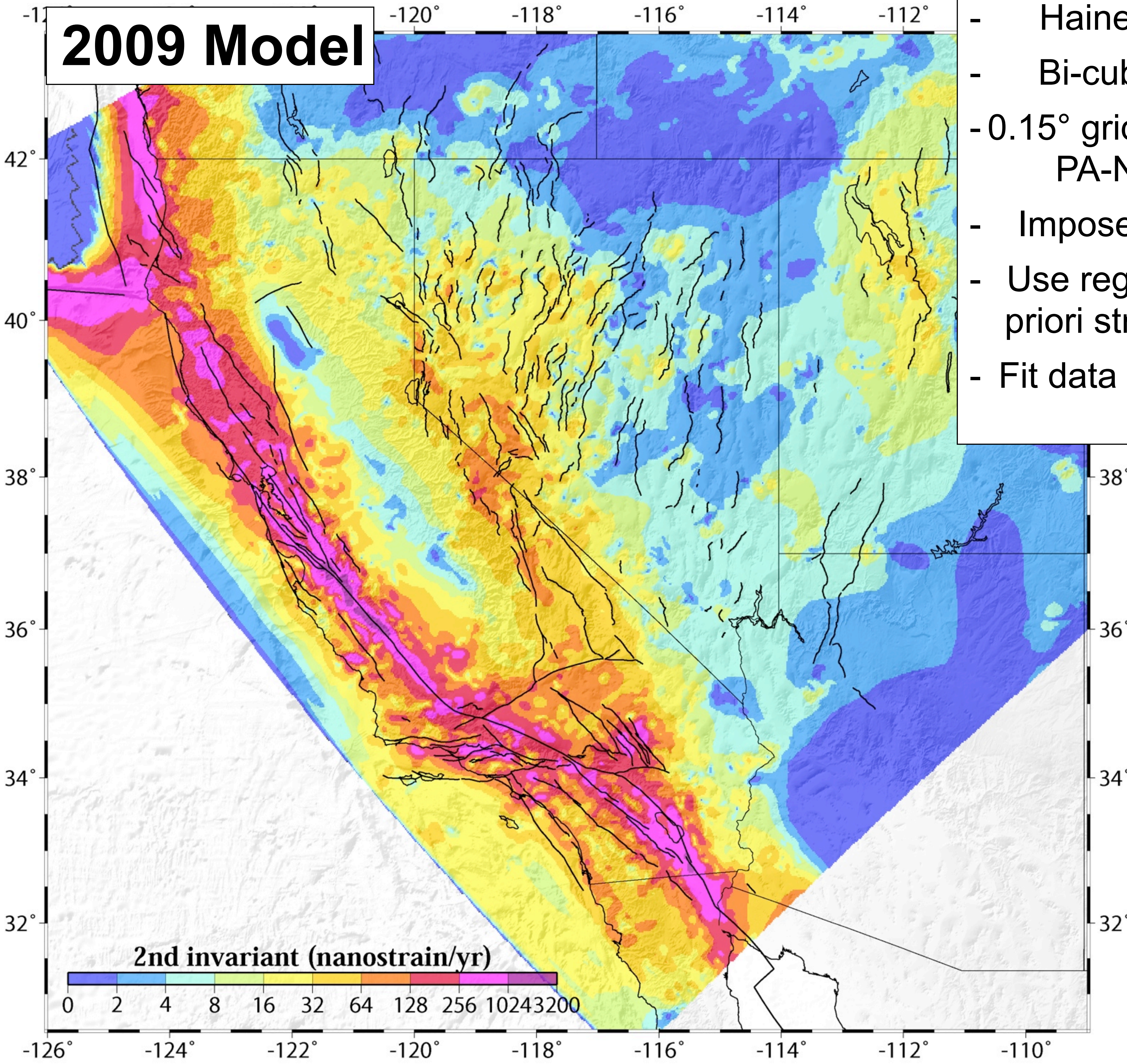

- Haines and Holt, 1993
- Bi-cubic Bessel splines
- 0.15° grid cells aligned along PA-NA small circles
- Imposed PA and JdF b.c.
- Use regions with variable a priori strain rate variances
- Fit data in each region to χ^2/dof ≈ 1

2009 Model

- Haines and Holt, 1993
- Bi-cubic Bessel splines
- 0.15° grid cells aligned along PA-NA small circles
- Imposed PA and JdF b.c.
- Use regions with variable a priori strain rate variances
- Fit data in each region to χ^2/dof ≈ 1

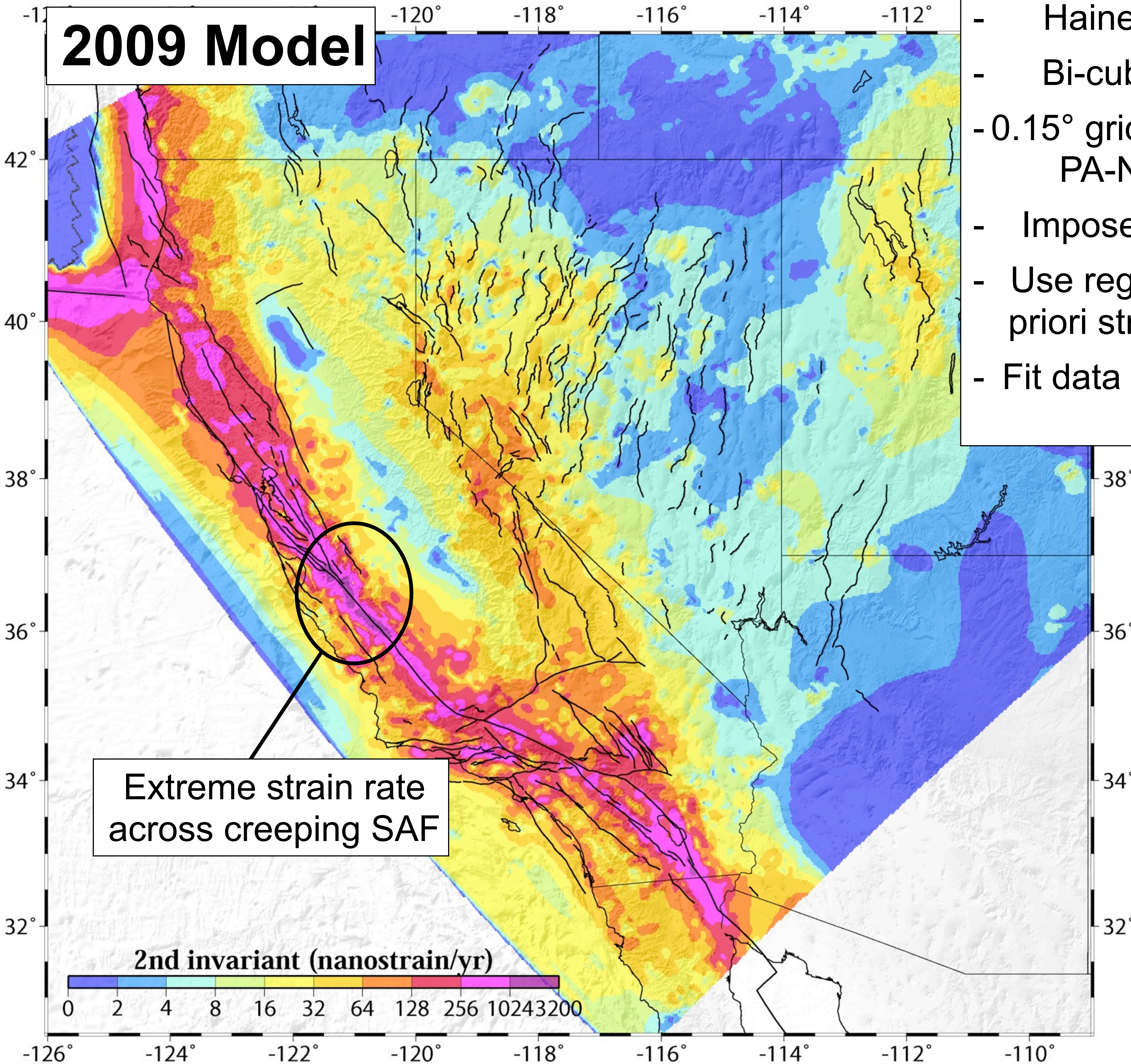

2009 Model

- Haines and Holt, 1993
- Bi-cubic Bessel splines
- 0.15° grid cells aligned along PA-NA small circles
- Imposed PA and JdF b.c.
- Use regions with variable a priori strain rate variances
- Fit data in each region to χ^2/dof ≈ 1

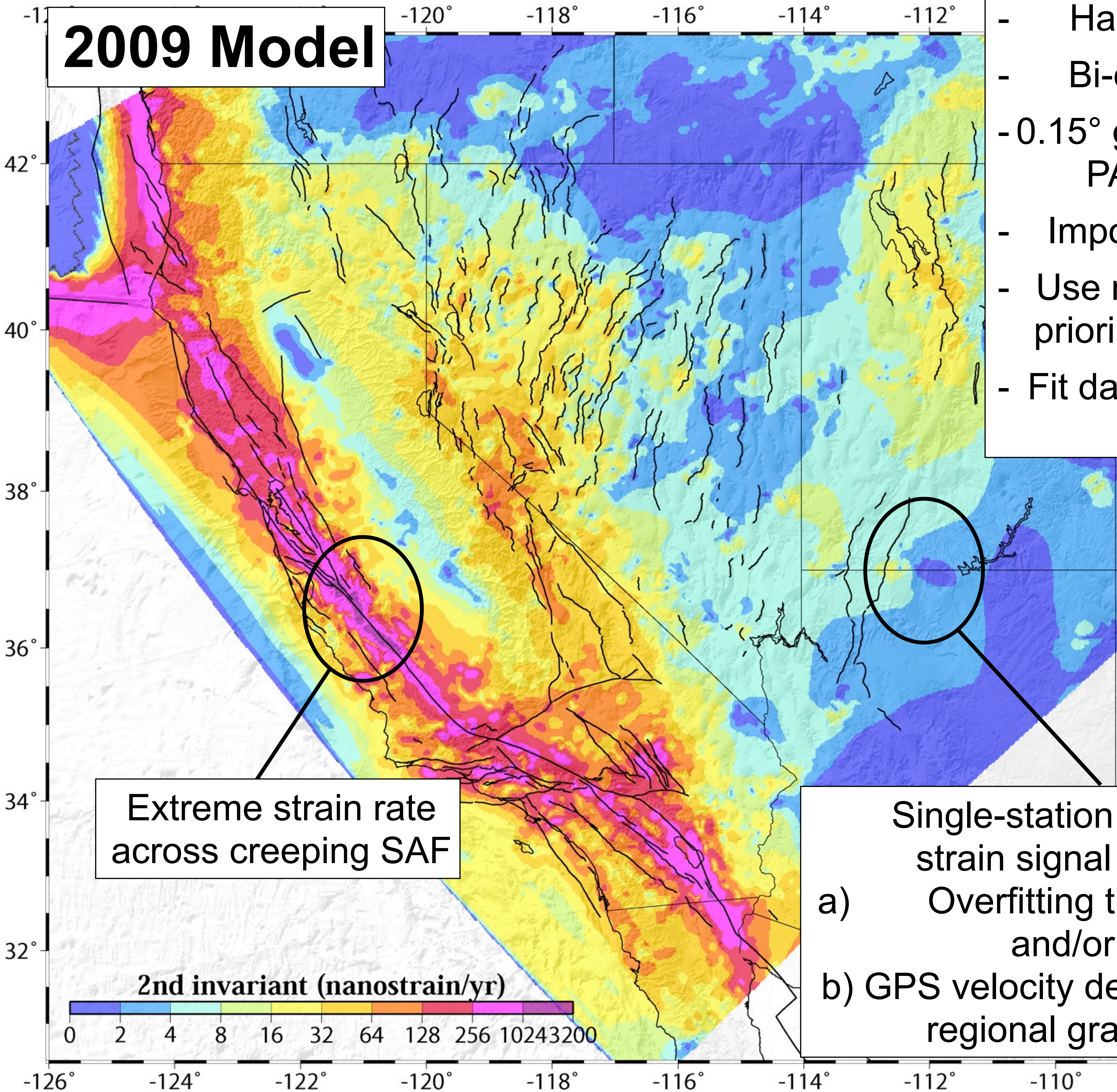

Extreme strain rate across creeping SAF

Single-station bi-lobe strain signal when
a) Overfitting the data and/or
b) GPS velocity deviates from regional gradient

- UNR analysis of CGPS (Red)
- UNR MAGNET (Blue)
- Published campaign velocities transformed into same NA-reference frame (Green)

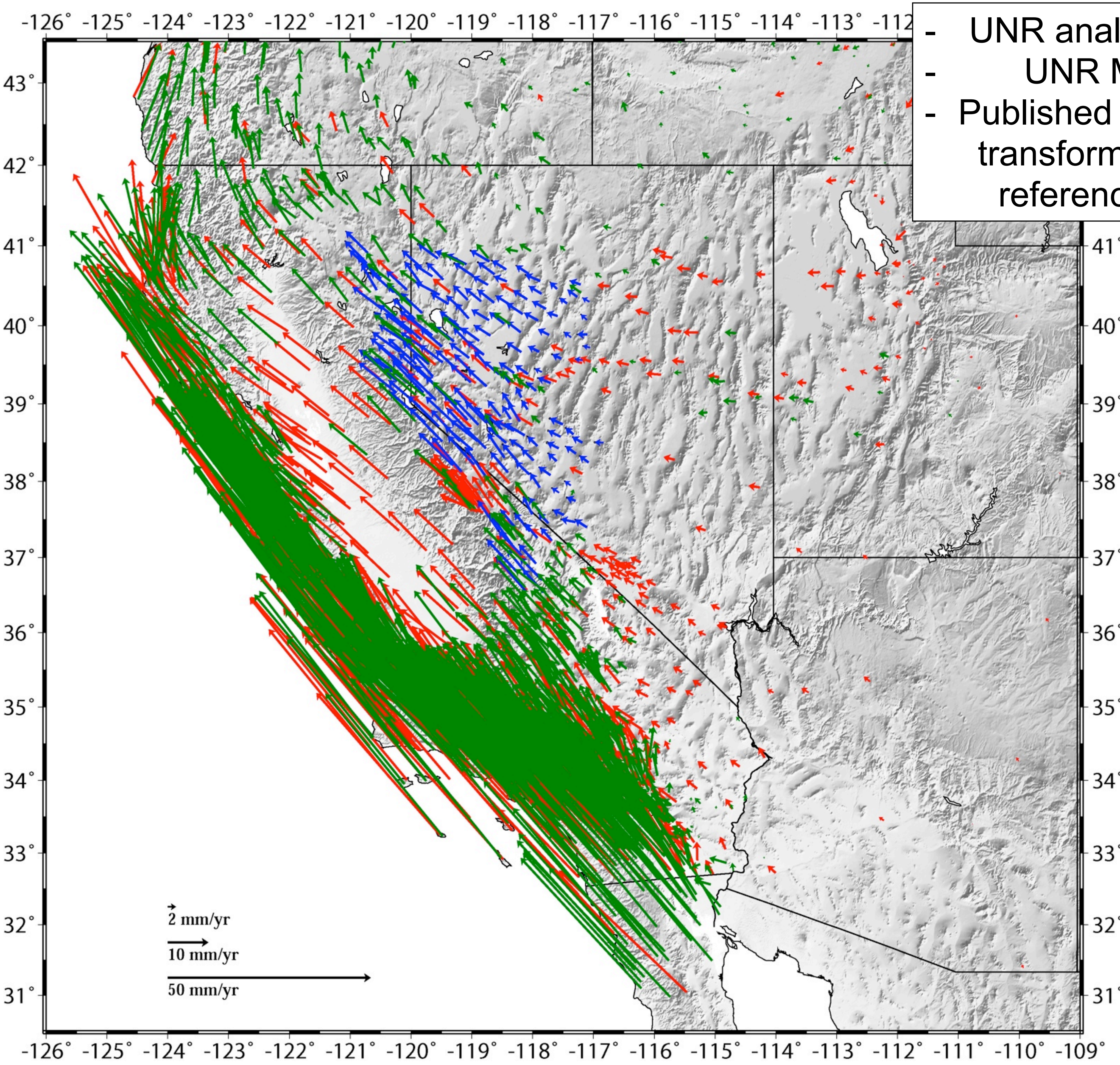

- UNR analysis of CGPS (Red)
- UNR MAGNET (Blue)
- Published campaign velocities transformed into same NA-reference frame (Green)

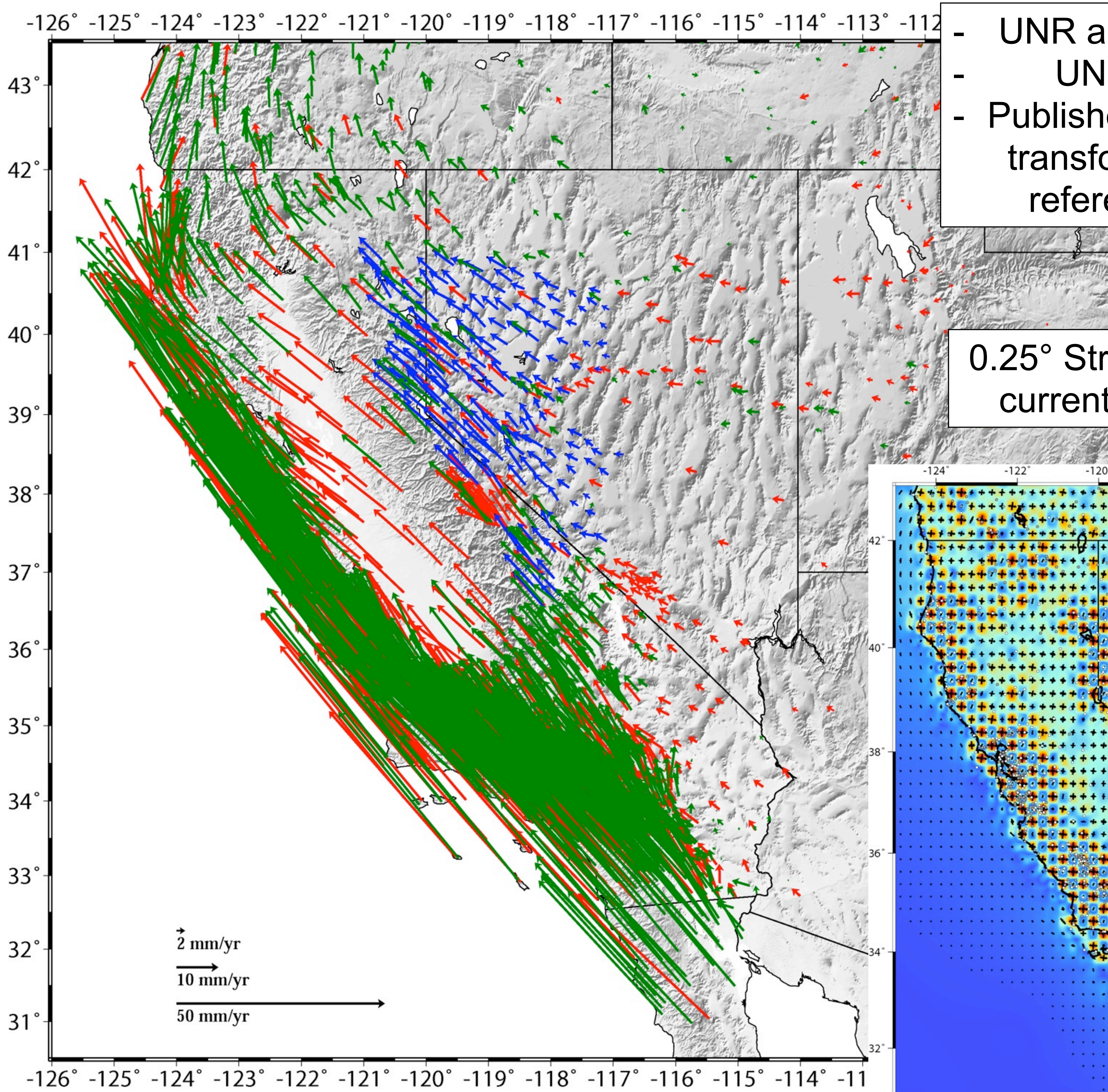

0.25° Strain resolution from current data distribution

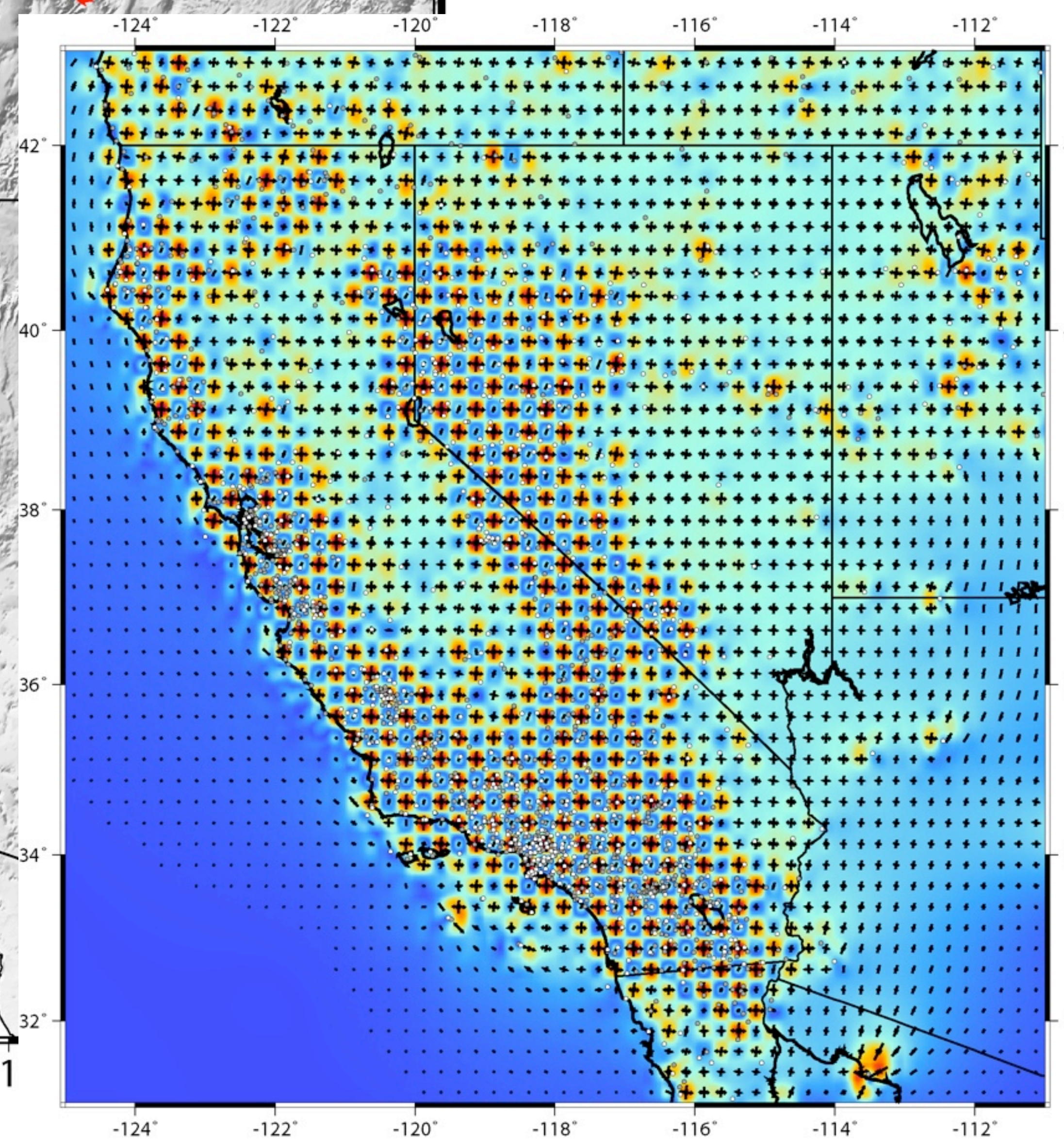

NEXT STEPS

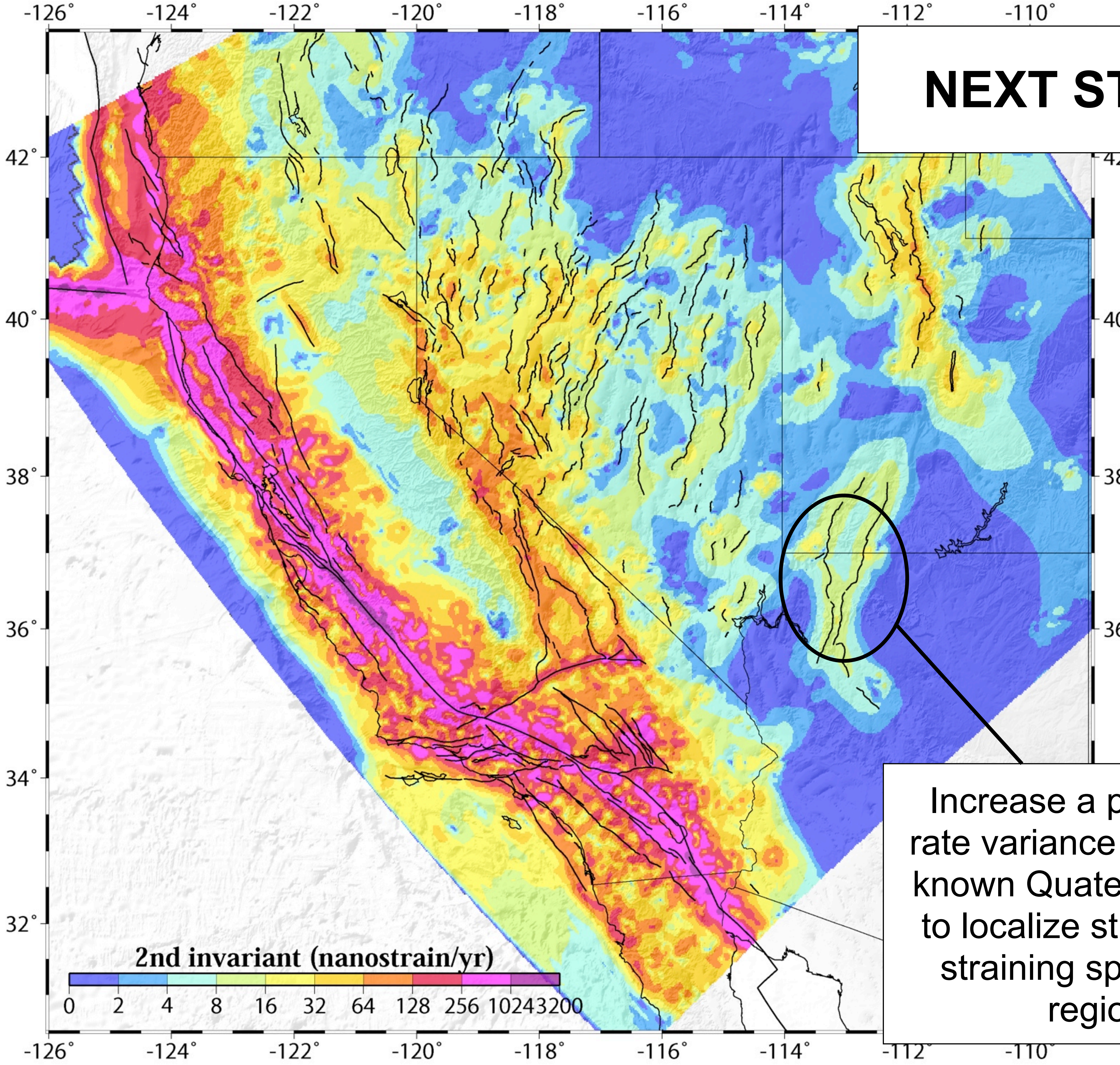

Increase a priori strain rate variance at traces of known Quaternary faults to localize strain in low-straining sparse data regions

NEXT STEPS

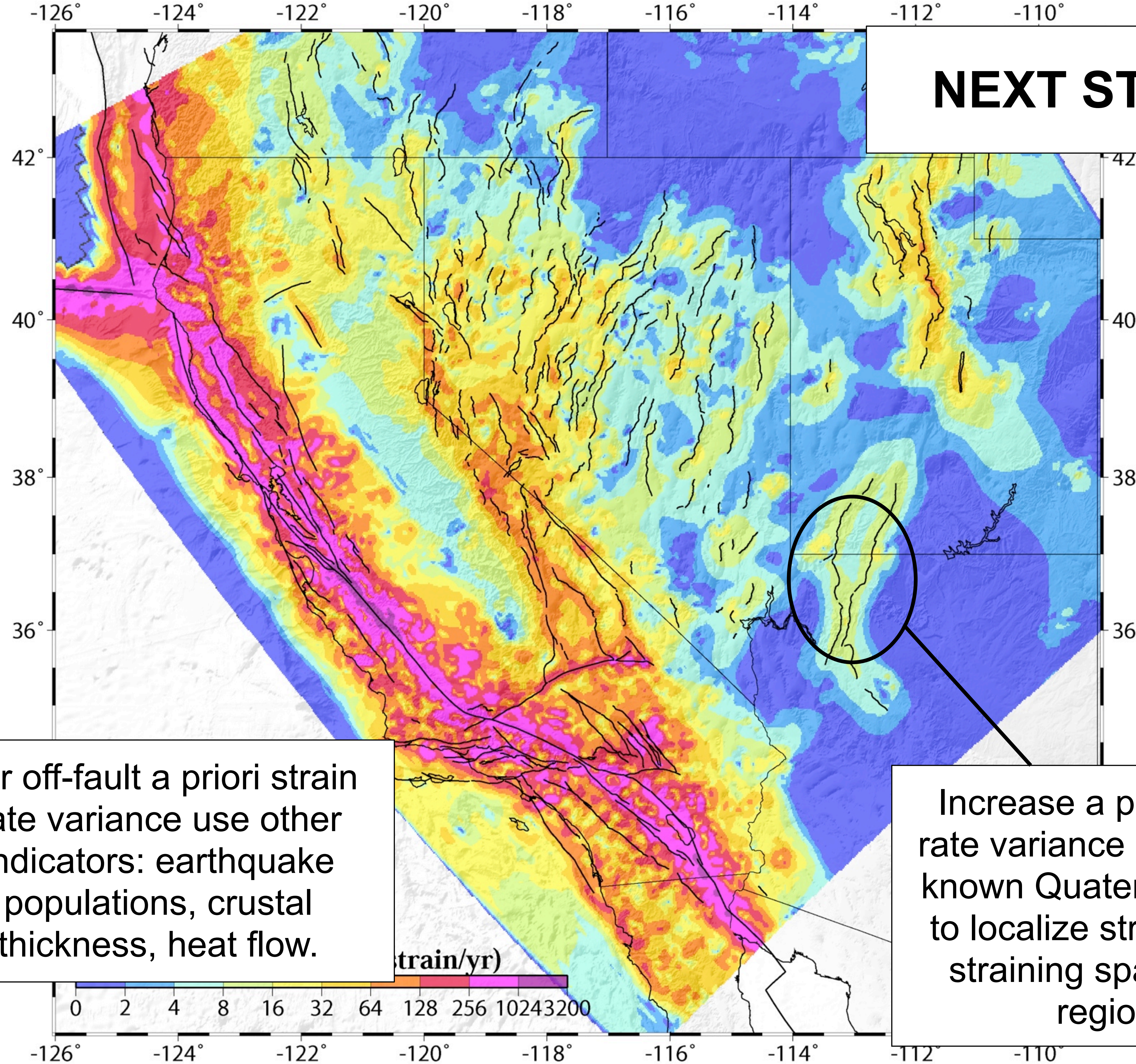

For off-fault a priori strain rate variance use other indicators: earthquake populations, crustal thickness, heat flow.

Increase a priori strain rate variance at traces of known Quaternary faults to localize strain in low-straining sparse data regions

NEXT STEPS

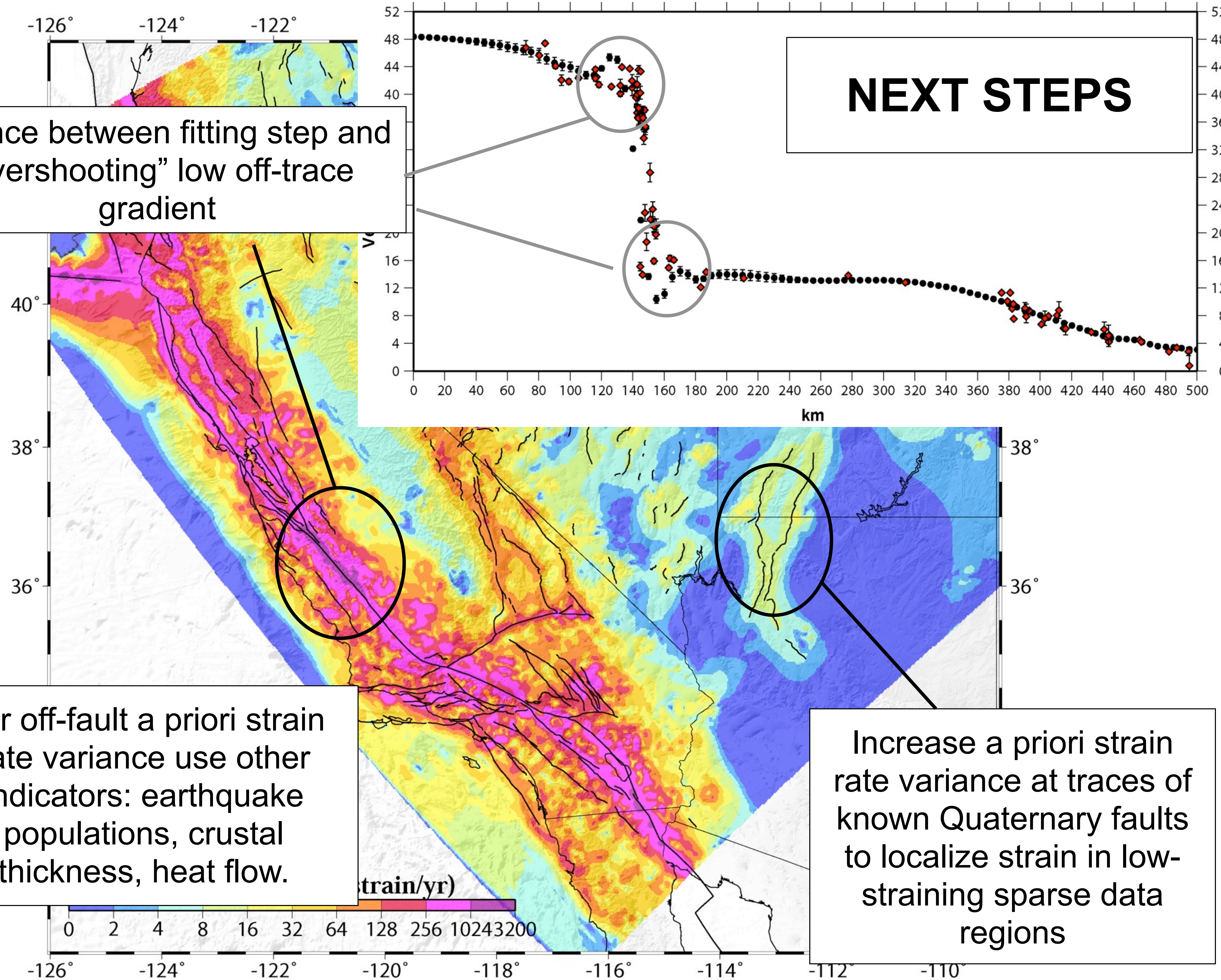

Balance between fitting step and "overshooting" low off-trace gradient

For off-fault a priori strain rate variance use other indicators: earthquake populations, crustal thickness, heat flow.

Increase a priori strain rate variance at traces of known Quaternary faults to localize strain in low-straining sparse data regions

Global Strain Rate Map

Kreemer et al. 2000 (see reading list) also see
http://gsrm.unavco.org/

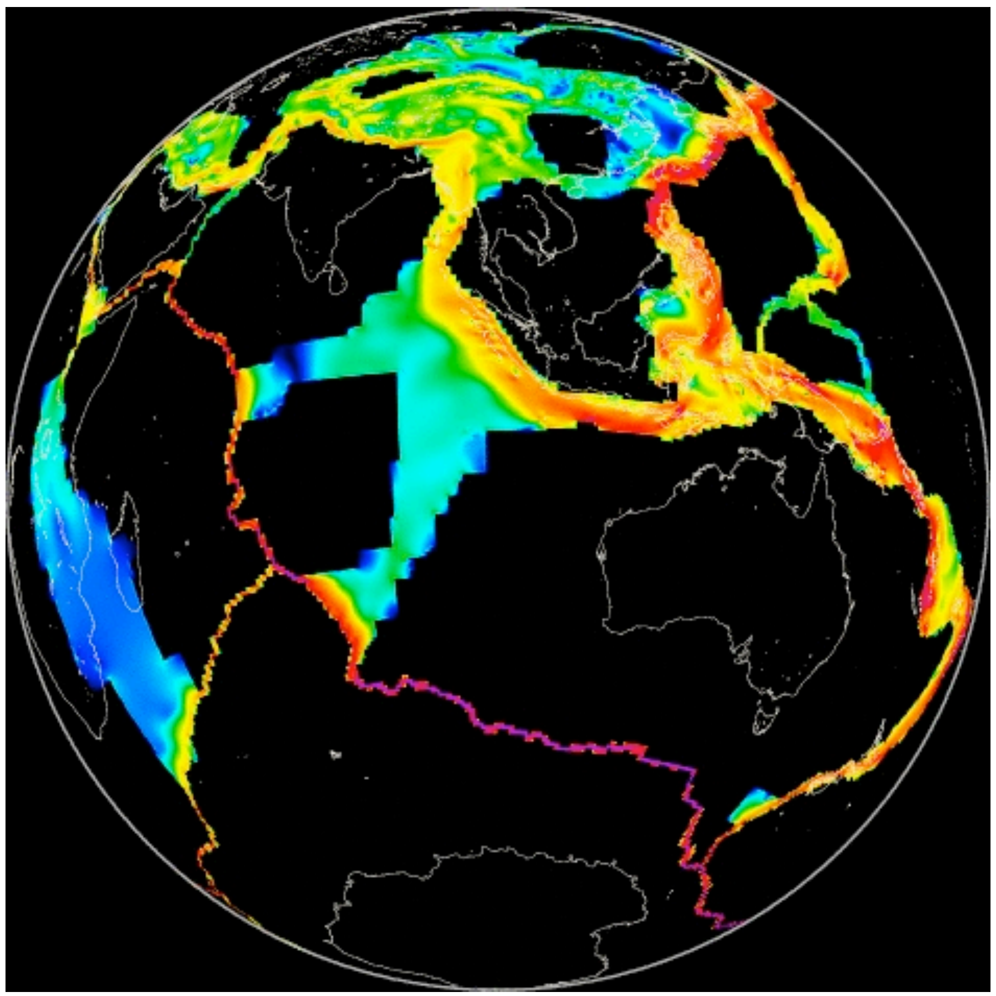

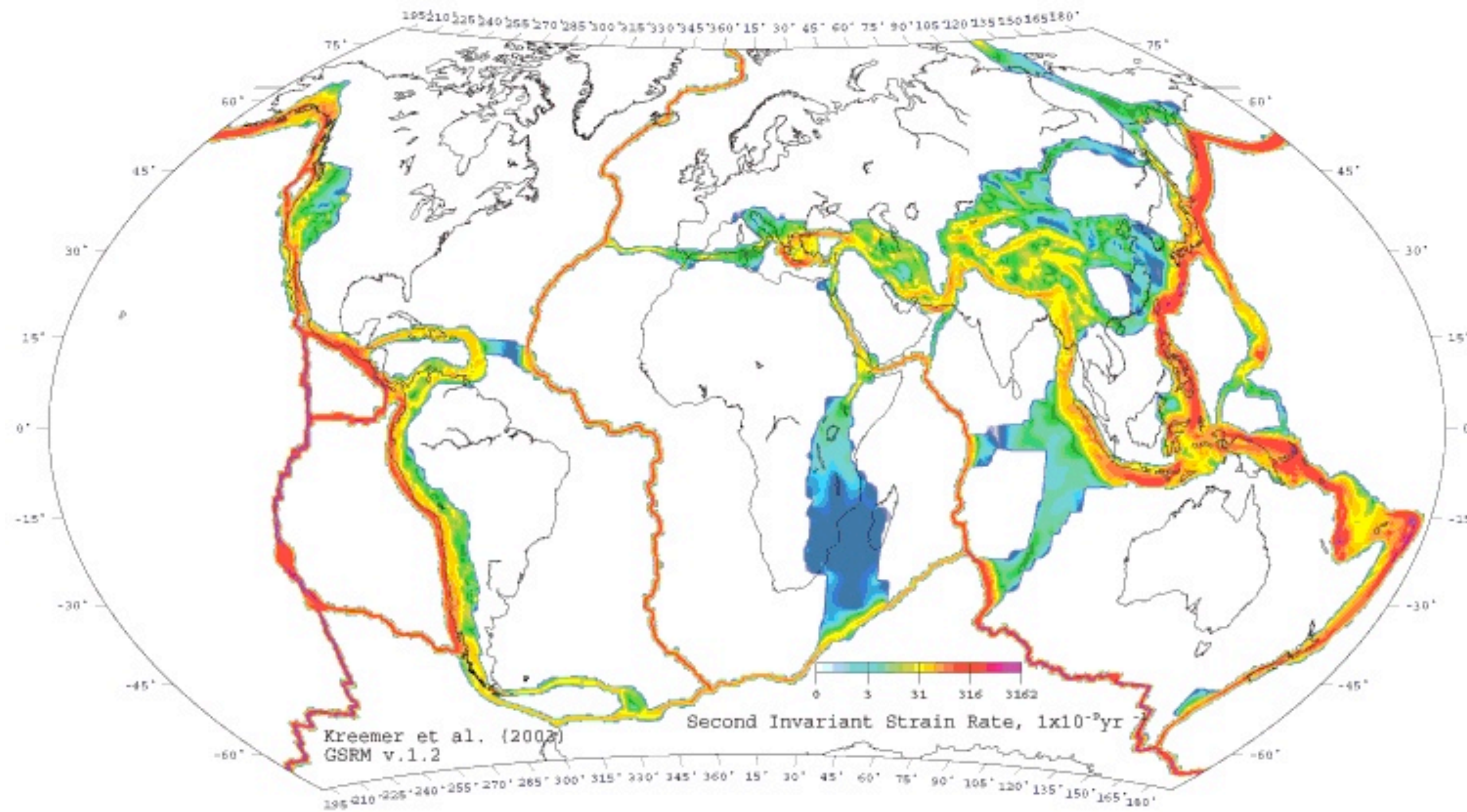

Kostrov Formula: Relating seismic or geologic moment release (rate) to geodetic strain accumulation (rate)

From Earthquakes

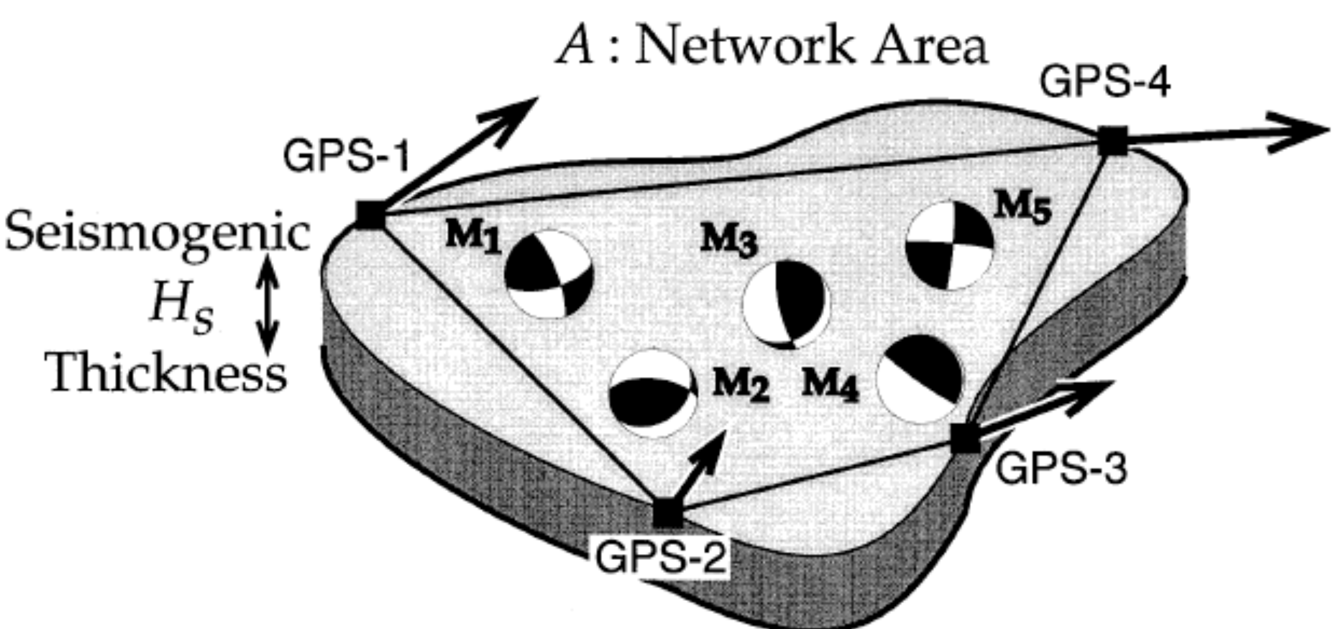

Kostrov (1974) $$2\mu A H_s \dot{\mathbf{e}} = (1/T) \sum_{n=1}^{m} \mathbf{M_n}$$

Figure 1. Cartoon illustrating the tie between the observed geodetic strain rate within a network of area A and the potential rate of seismic moment release. Kostrov's (1974) linear relationship between tensor strain rate and moment rate hinges on parameter H_s, the seismogenic thickness.

(from Ward, 1998)

From Faults

Observed average seismic strain rates for any grid area can be obtained by summing moment tensors in the volume described by the product of the grid area and the assumed seismogenic thickness (Kostrov, 1974);

$$\dot{\varepsilon}_{ij} = \frac{1}{2\mu V T} \sum_{k=1}^{N} M_0 m_{ij}, \tag{2}$$

where N is the number of events in the grid area, μ is the shear modulus, V the cell volume, T is the time period of the earthquake record, M_0 is the seismic moment, and m_{ij} is the unit moment tensor. Similarly, average horizontal strain rate components from Quaternary fault slip data are obtained by a variant of Kostrov's (1974) summation;

$$\dot{\varepsilon}_{ij} = \frac{1}{2} \sum_{k=1}^{n} \frac{L_k \dot{u}_k}{A \sin \delta_k} m_{ij}^{k}, \tag{3}$$

where m_{ij} is the unit moment tensor defined by the fault orientation and unit slip vector, and n is the number of fault segments in grid area A, each having a length L_k, dip angle δ_k, and slip rate $\dot{u}_k$.

Block Models

- What are they: A way to interpret geologic and geodetic data in terms of crustal deformation and seismic hazard
- Interseismic vs. coseismic vs. postseismic: Time
- What do block models assume?
  - Velocity data are representative of interseismic motion
  - Enforces kinematic self-consistency in modeling
  - Faults are locked at surface and slipping at depth
  - Block geometries must be right, i.e. interiors are rigid over ‘long-term’ and deformation on faults occurs during earthquakes
- The Goal:
  - Slip rates on block-bounding faults over a geologically significant period of time. How long is that?
- Transients

"Long Term" Velocity = Interseismic + Coseismic Velocity

$$\vec{v}_{LT} = \vec{v}_{Int} + \vec{v}_{Cos}$$

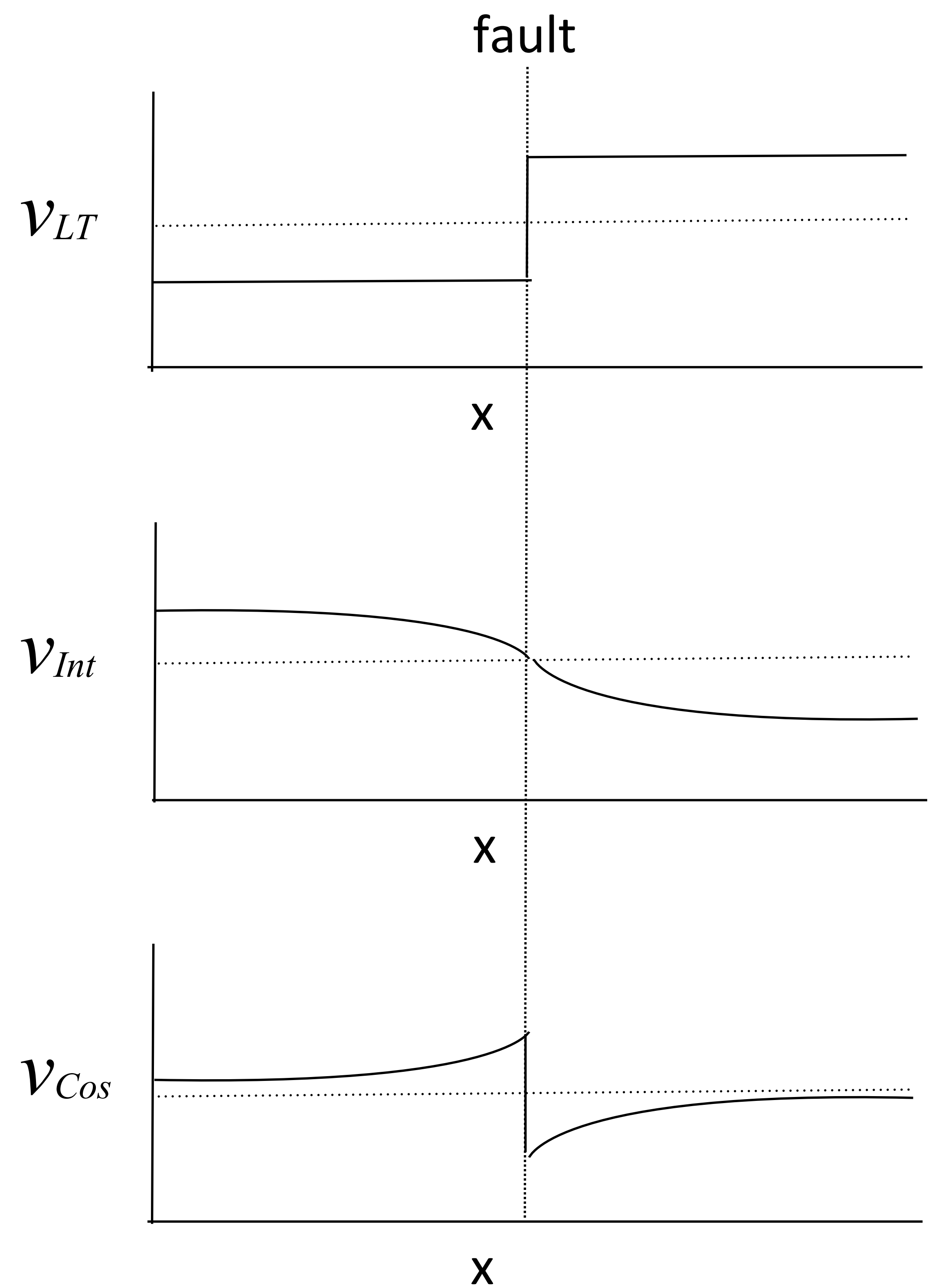

Block Modeling Theory

$$\vec{v}_{LT} = \vec{v}_{Int} + \vec{v}_{Cos}$$

$$\vec{v}_{Int} = \vec{v}_{LT} - \vec{v}_{Cos}$$

Solve for Block rotations: ω_j , and slip rates a_k, b_k

$$\vec{v}_{GPS,i} = \vec{\omega}_j \times \vec{r}_i - (a_k \vec{G}_{ss,k} + b_k \vec{G}_{N,k})$$

Constraint: Block motions consistent with slip rates

$$\vec{\omega}_{j_1} \times \vec{p}_k - \vec{\omega}_{j_2} \times \vec{p}_k = a_k \delta \vec{G}_{SS,k} + b_k \delta \vec{G}_{N,k}$$

Damping $\vec{\omega}_j = c$ $a_k = c$ $b_k = c$

Northern Walker Lane Velocity Field from MAGNET/PBO/BARGEN

(North America Frame)

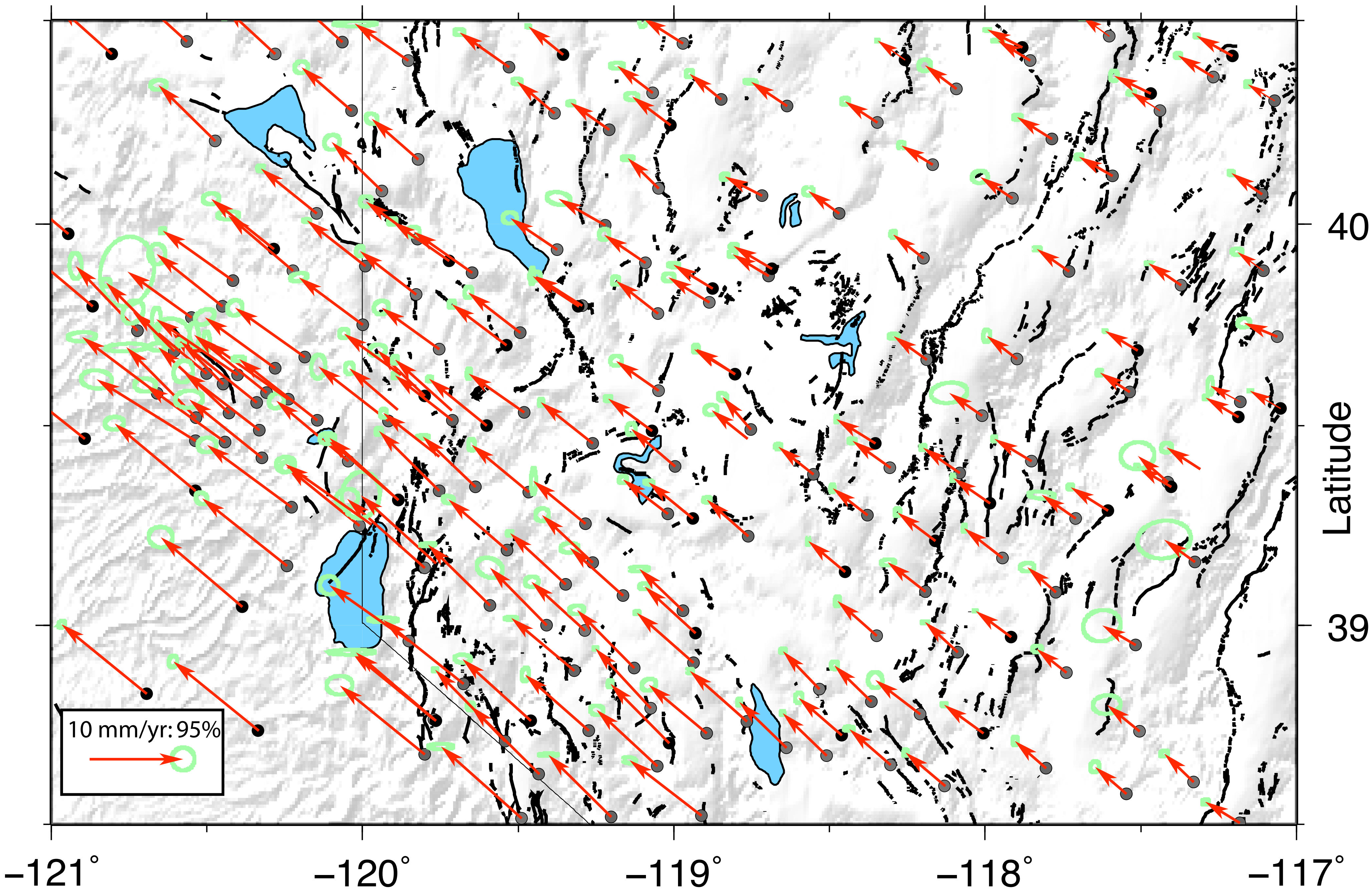

- 199 velocities
- 20 km spacing or less
- Up to 5 years of MAGNET + PBO
- Great Basin scale region filtering
- Uncertainties with CATS
- Velocity field *not* oversampled
- SNGV rigid

Northern Walker Lane Velocity Field from MAGNET/PBO/BARGEN

(Sierra Nevada Frame)

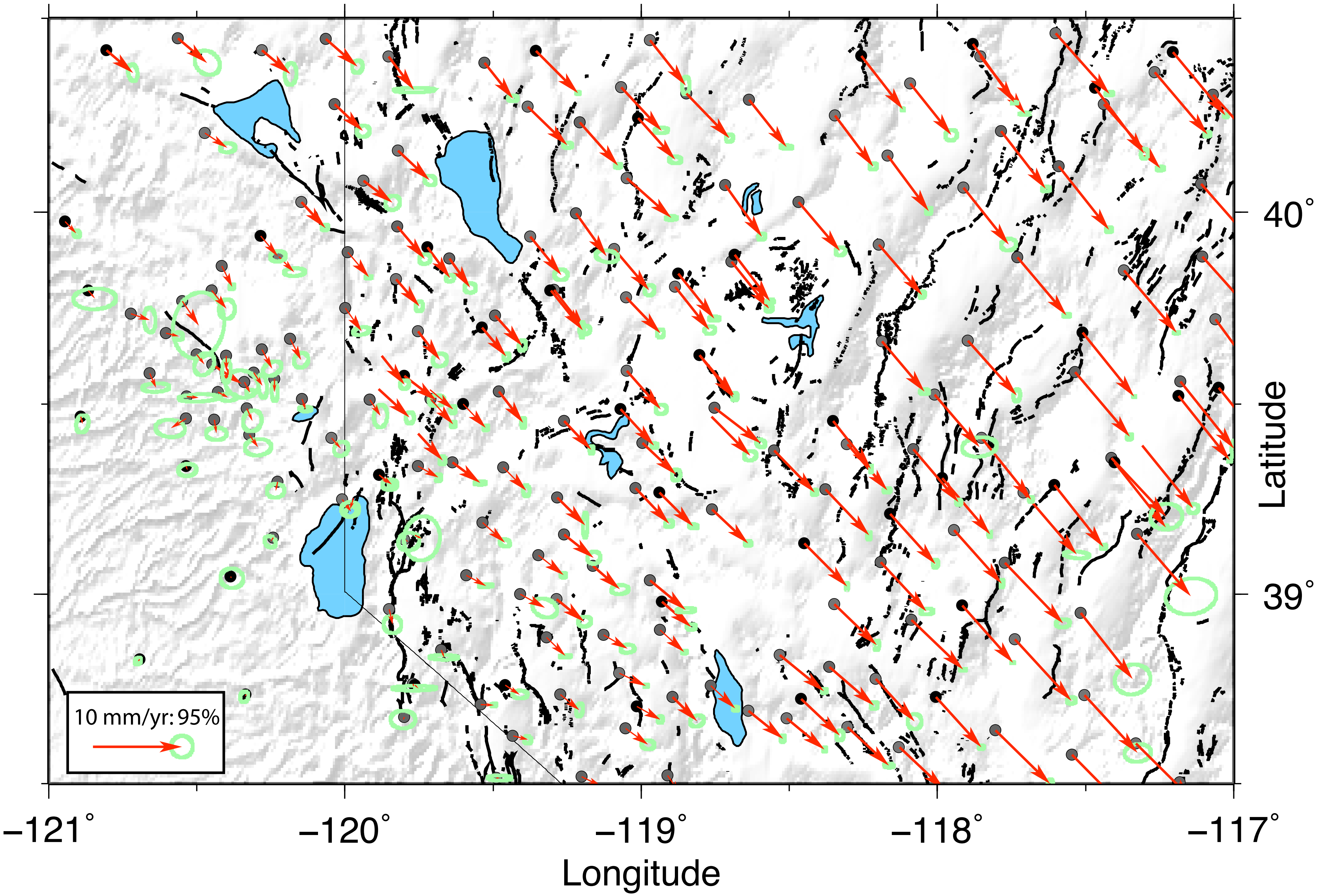

- 199 velocities
- 20 km spacing or less
- Up to 5 years of MAGNET + PBO
- Great Basin scale region filtering
- Uncertainties with CATS
- Velocity field *not* oversampled
- SNGV rigid

Block Model: Displacement and Rotations

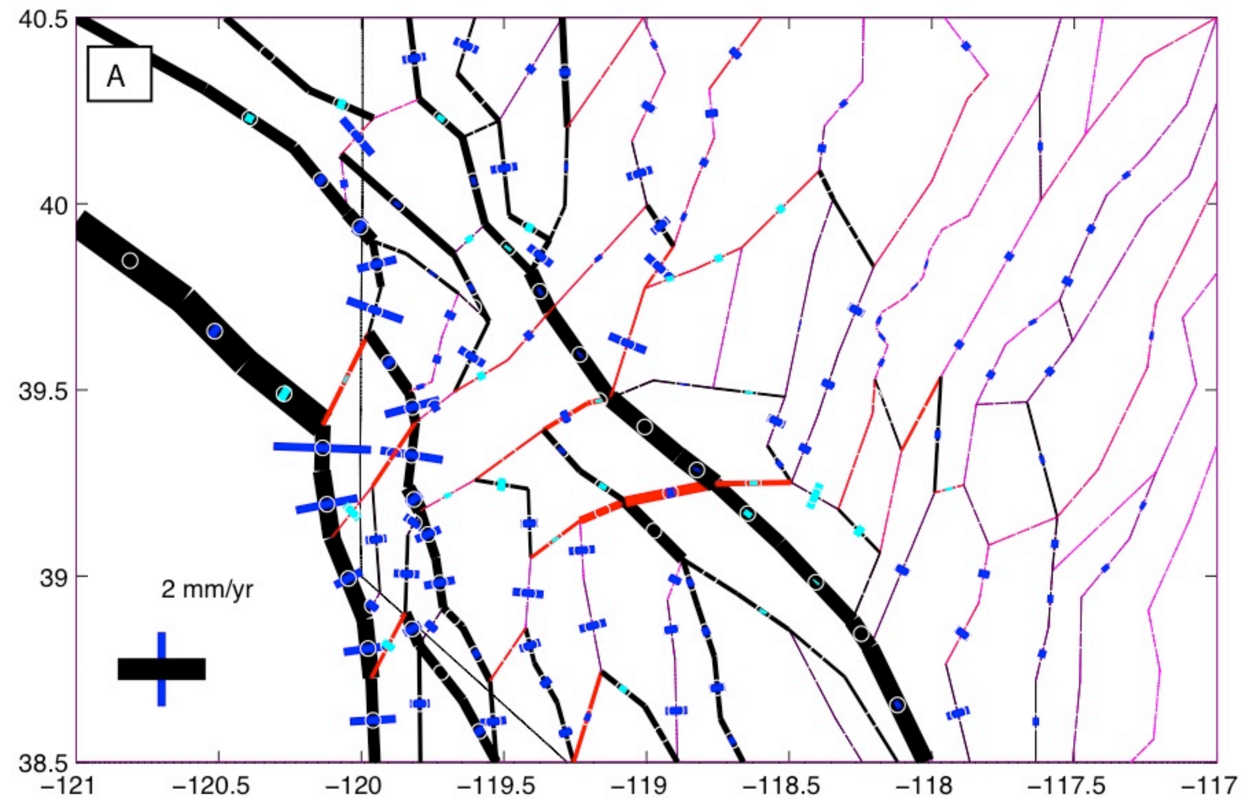

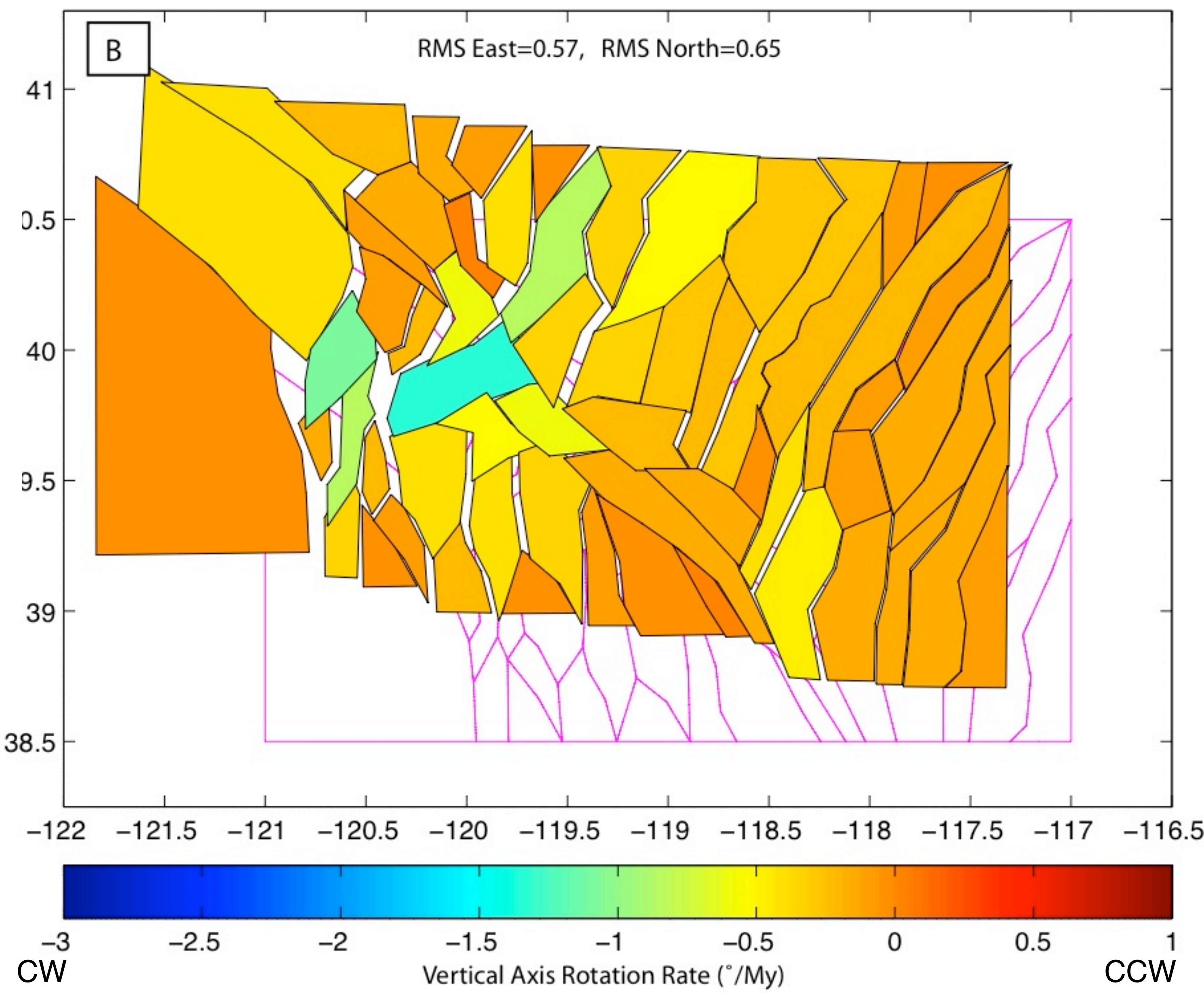

- Complementary views
- Constraints: data, slip rate damping, vertical axis rotation damping, slip rate/block motion consistency
- RMS velocity misfit ~0.6 mm/yr
- Intriguing rotation of Carson Domain
- Postseismic correction applied – See Poster

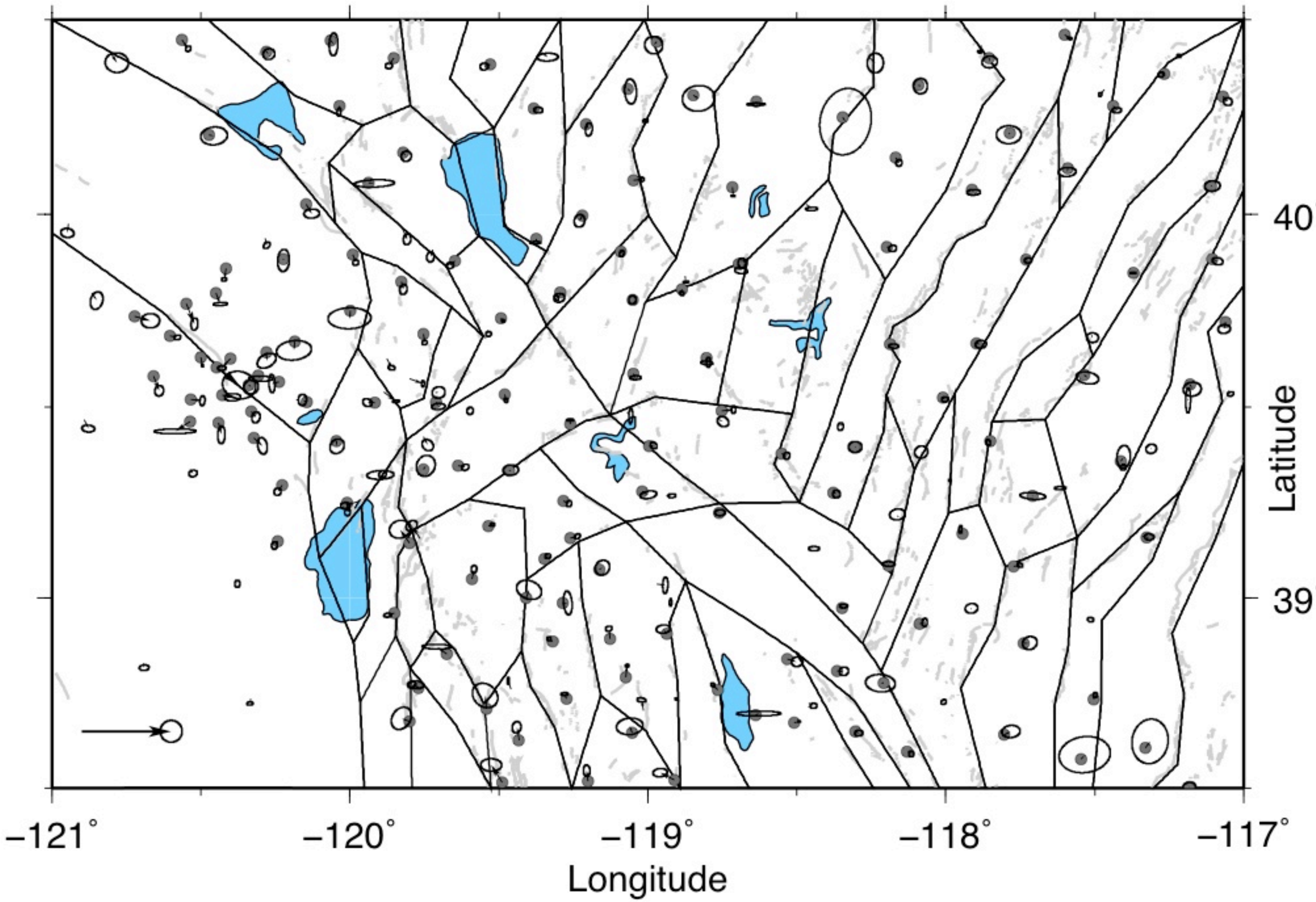
40°
39°
Latitude
−121°
−120°
−119°
−118°
−117°
Longitude

Northern Walker Lane Strain vs. Blocks vs. Hybrid Models

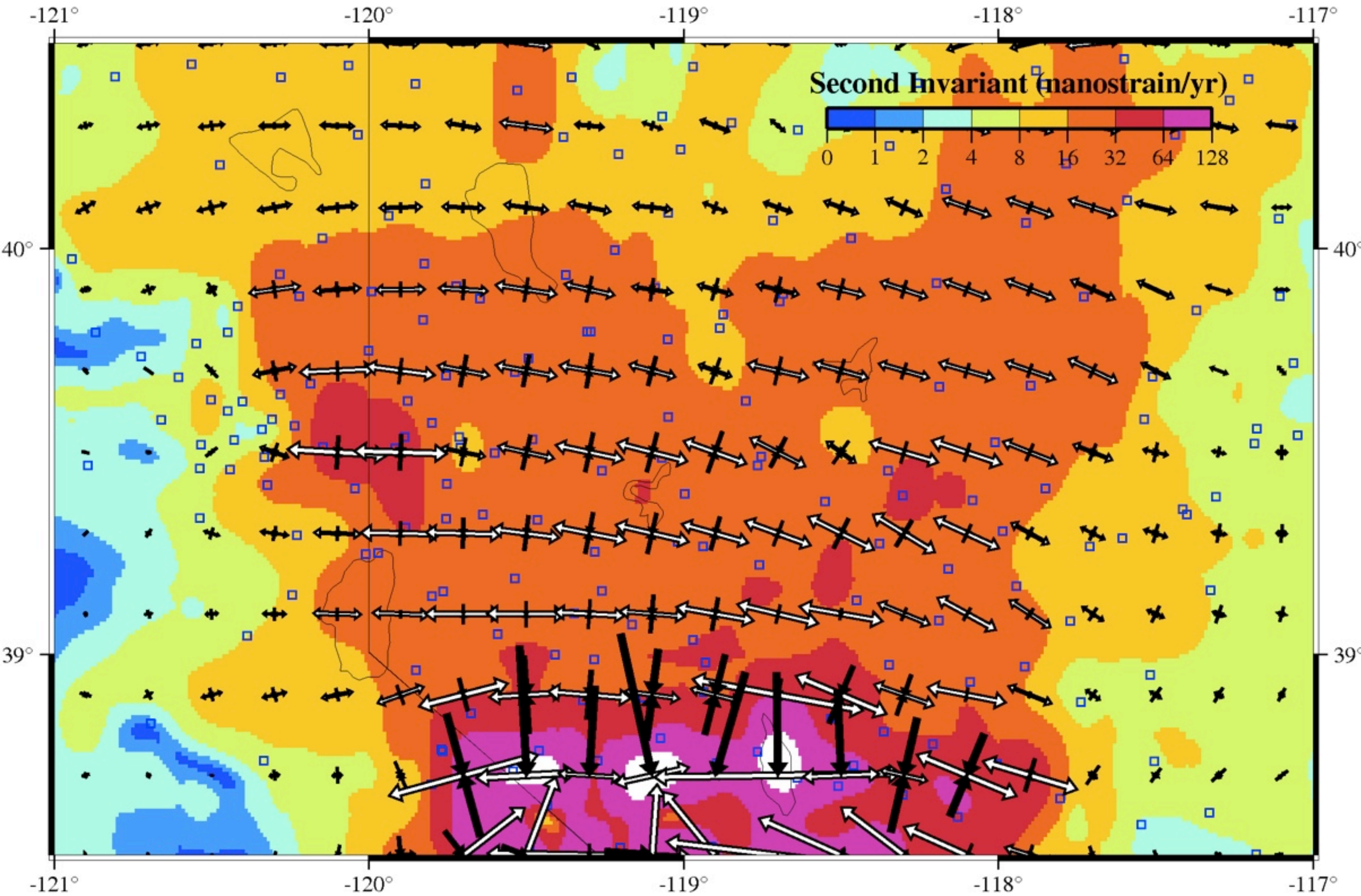

Strain rate from interpolation

Northern Walker Lane Strain vs. Blocks vs. Hybrid Models

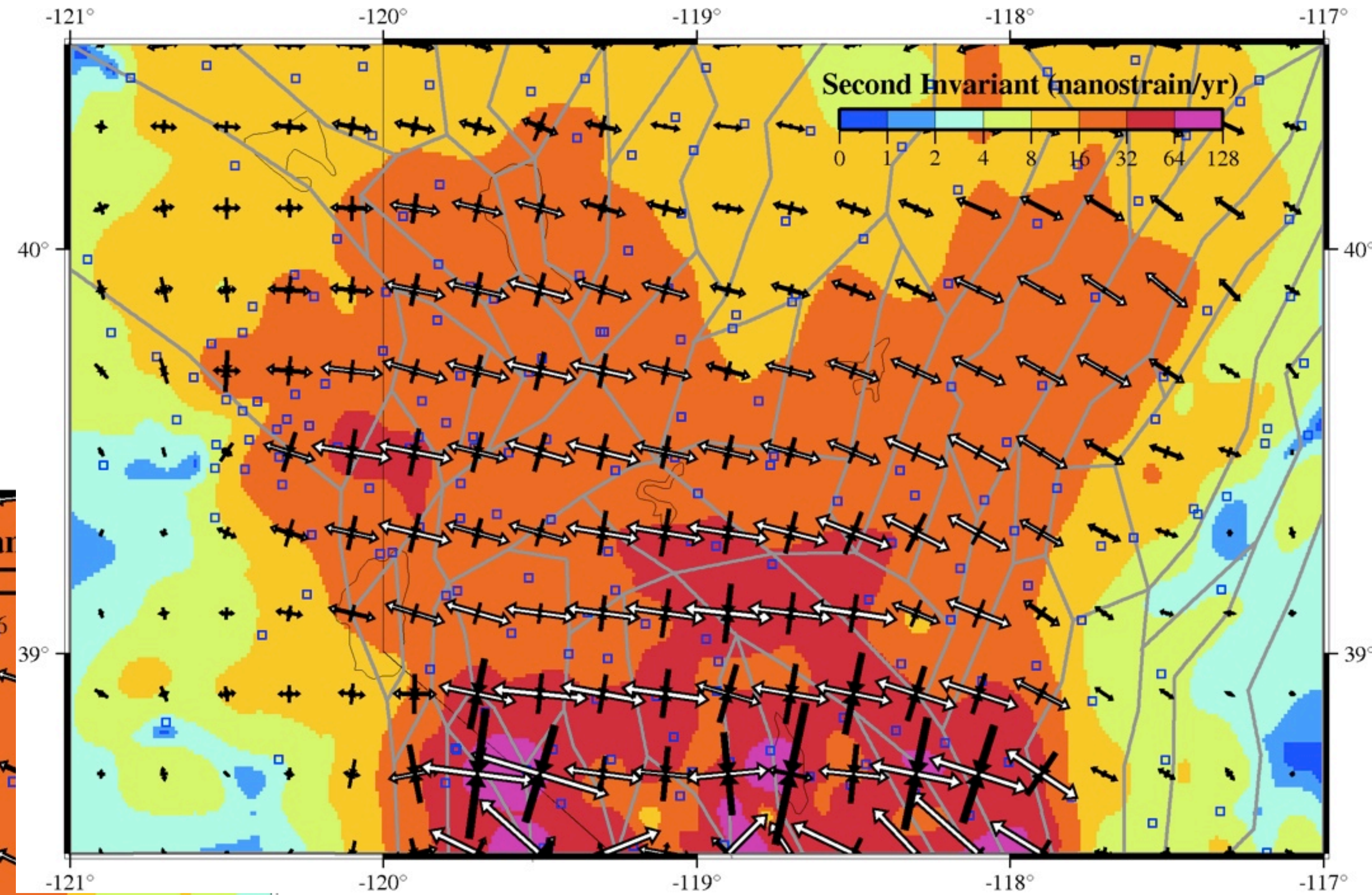

Strain rate from velocities at GPS sites predicted from block model

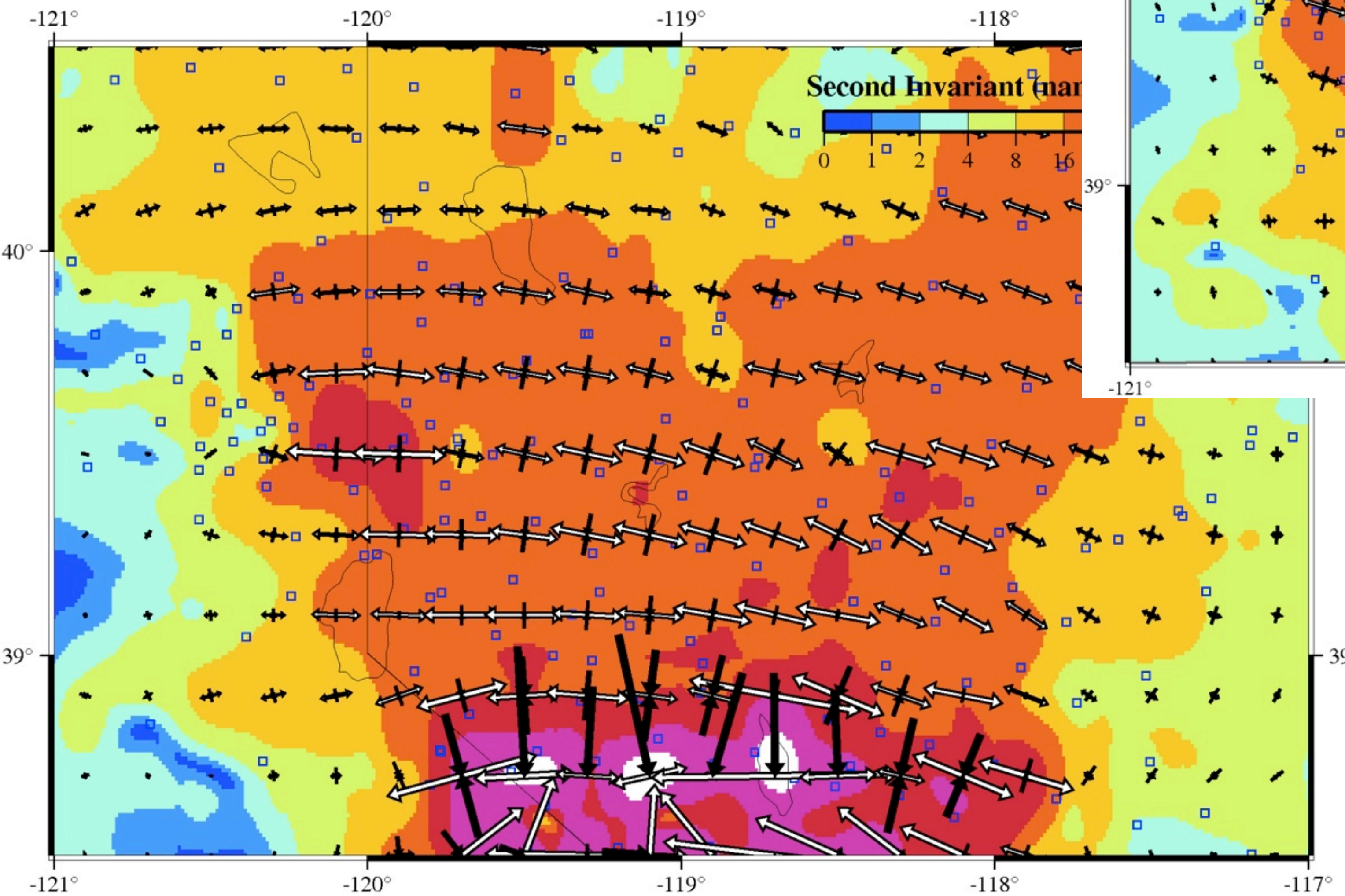

Strain rate from interpolation

Northern Walker Lane Strain vs. Blocks vs. Hybrid Models

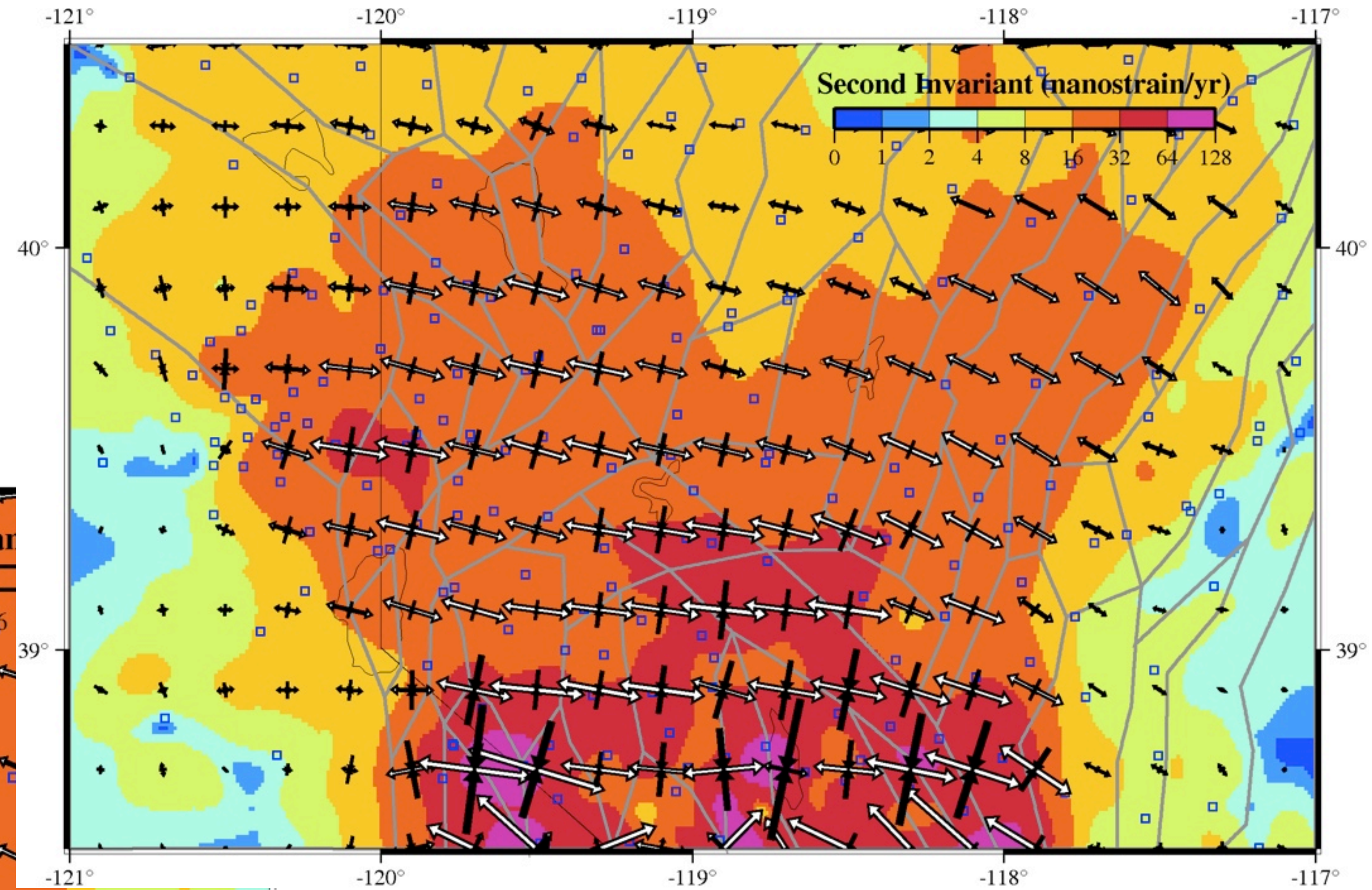

Strain rate from velocities at GPS sites predicted from block model

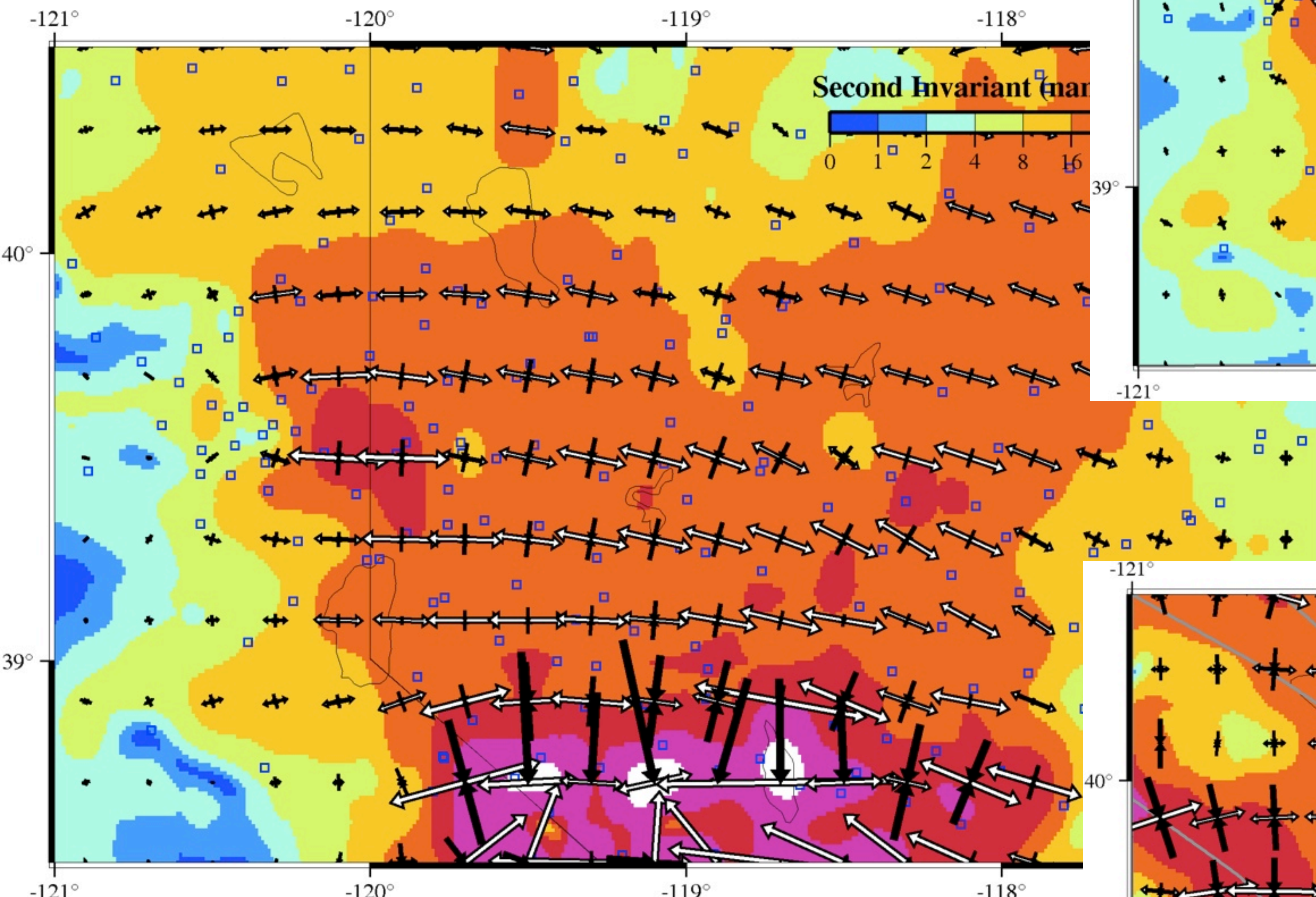

Strain rate from interpolation

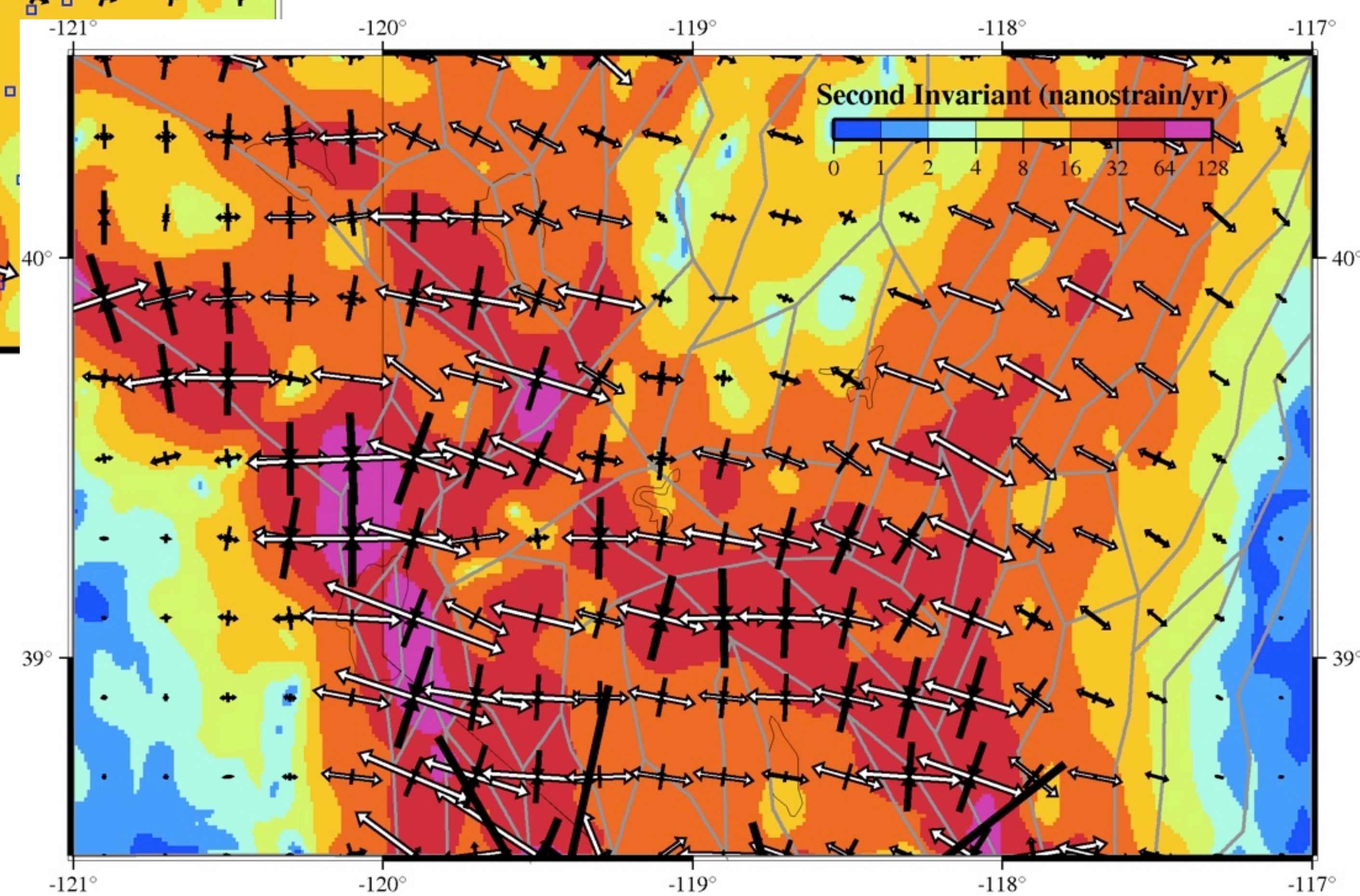

Strain rate from velocities at 0.1° grid predicted from block model

Meade and Hagar, 2005

Southern California

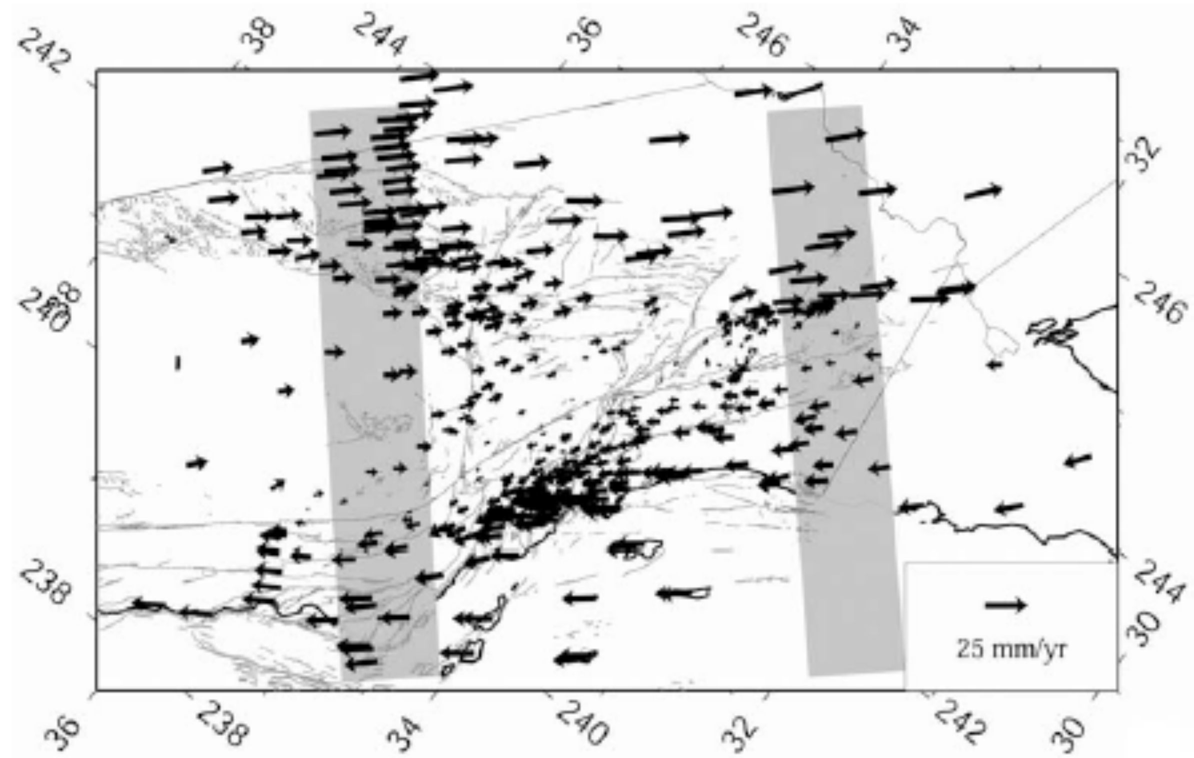

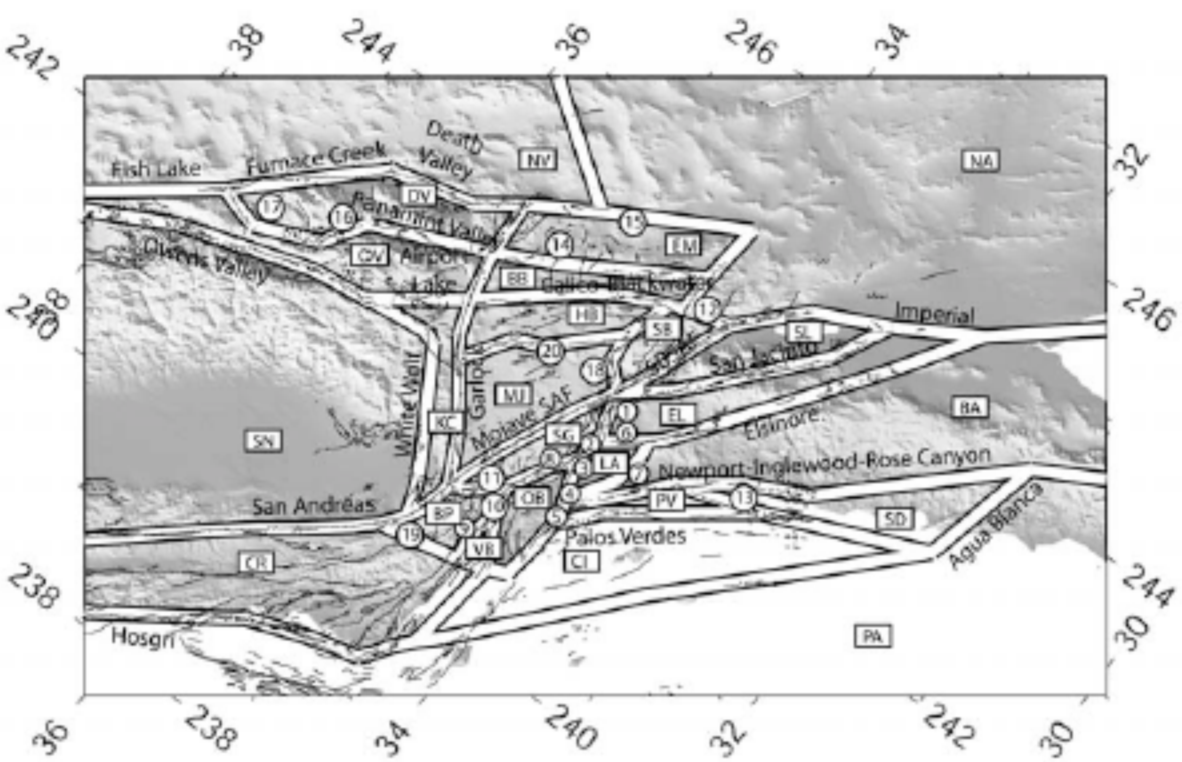

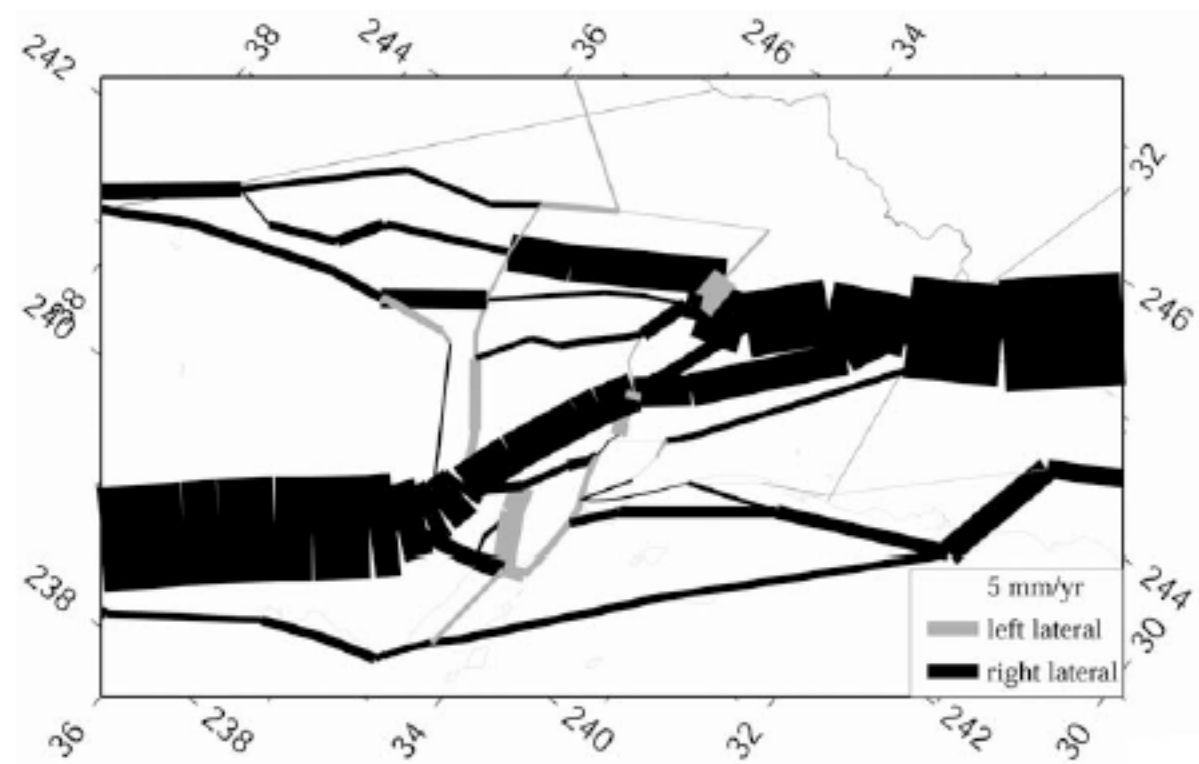

McCaffrey et al., 2007

Pacific Northwest

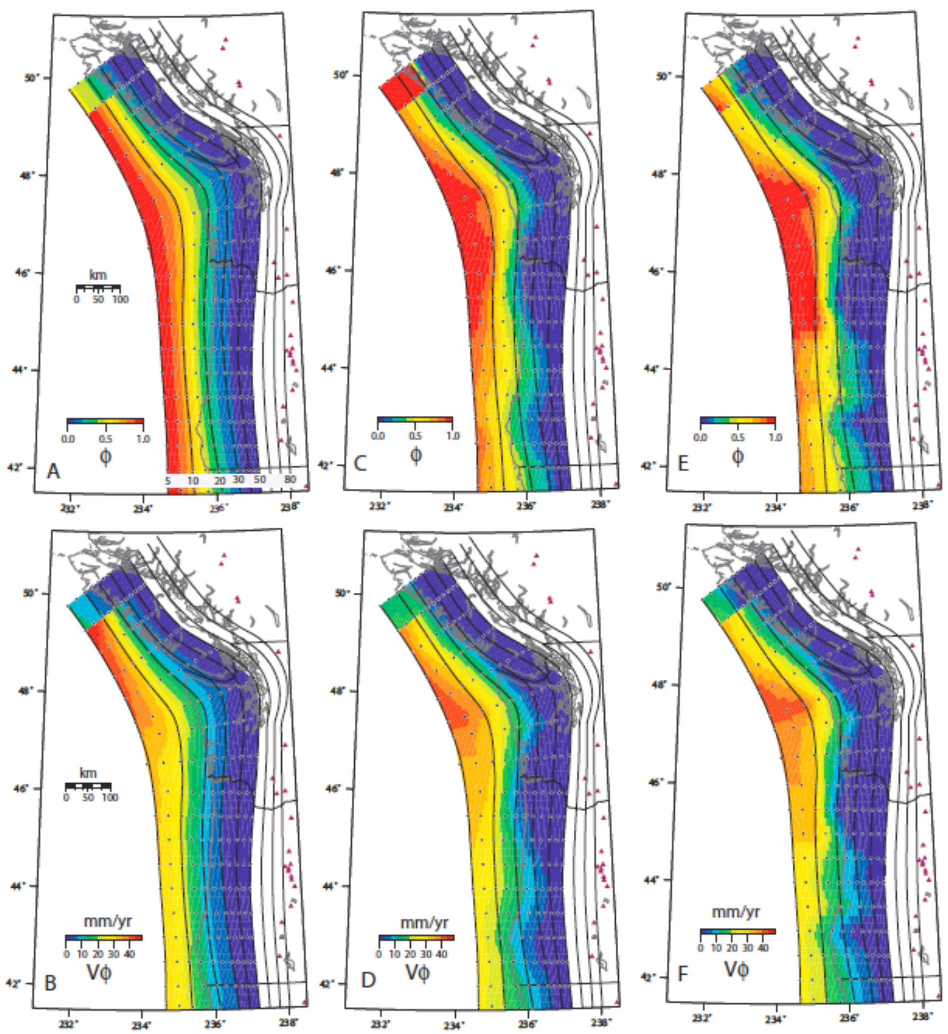

CM	Coast Mountains-generalized
SCF	Straight Creek Fault
DMF	Devil's Mountain Fault
JDF	Straits of Juan de Fuca faults
SWF	South Whidbey Island Fault
SF	Seattle Fault
WR	West Rainier seismic zone
ES	Entiat-Saddle Mountains faults
DF	Doty Fault
TK	Toppenish-Kittitas faults
WMF	Wallula-Milton Freewater
PH	Portland Hills fault
SH	Saint Helens seismic zone
LG	Le Grande graben
CF	Corvallis fault
KCG	Klamath-Chemult-Green Ridge graben
BF	Brothers Fault zone
LPB	Long Valley-Pine Valley-Baker
AGS	Abert-Goose Lake-Surprise Valley faults
SQO	Santa Rosa-Quinn-Owyhee faults
LRHL	Lost River-Hegben Lake faults

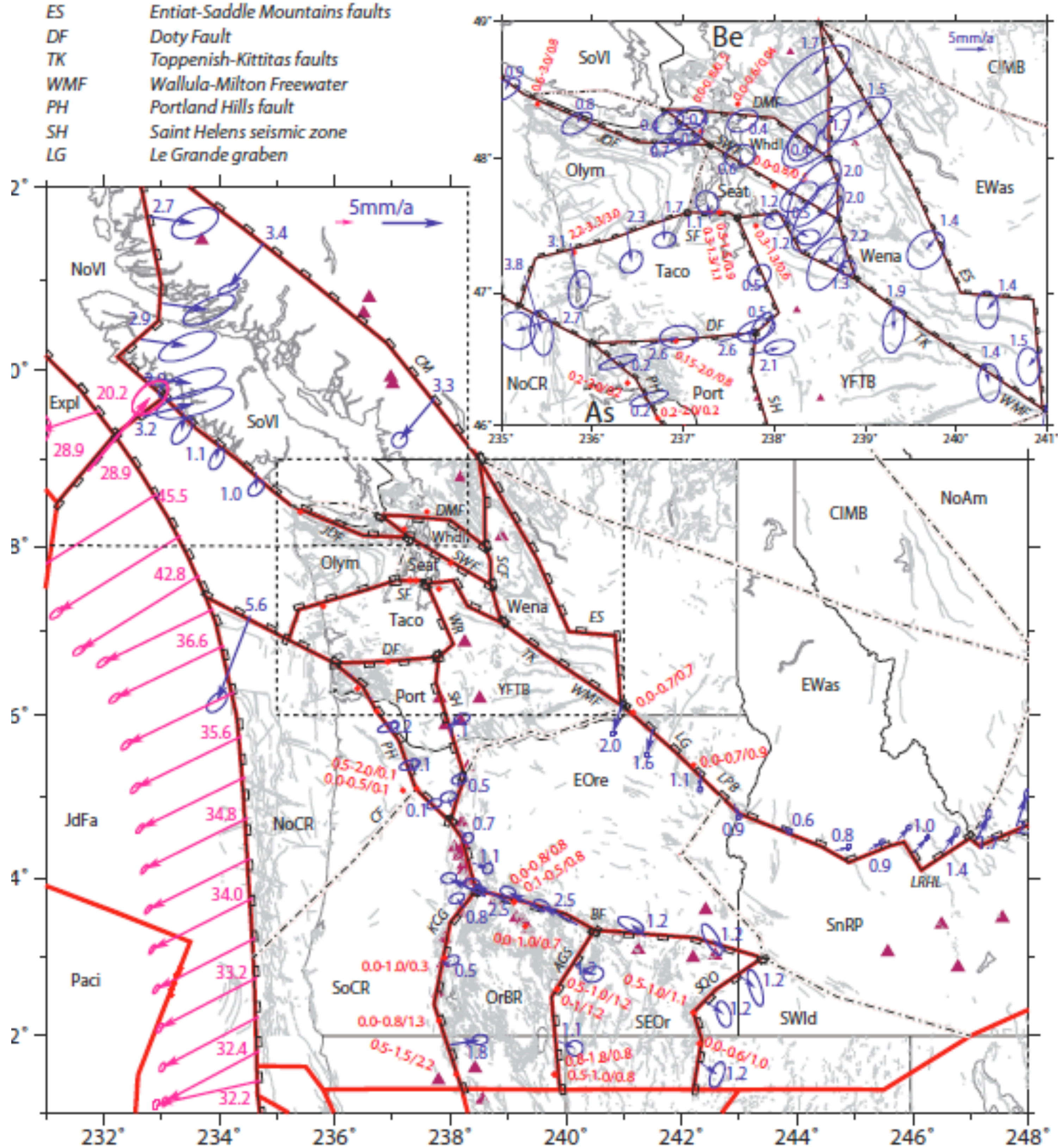

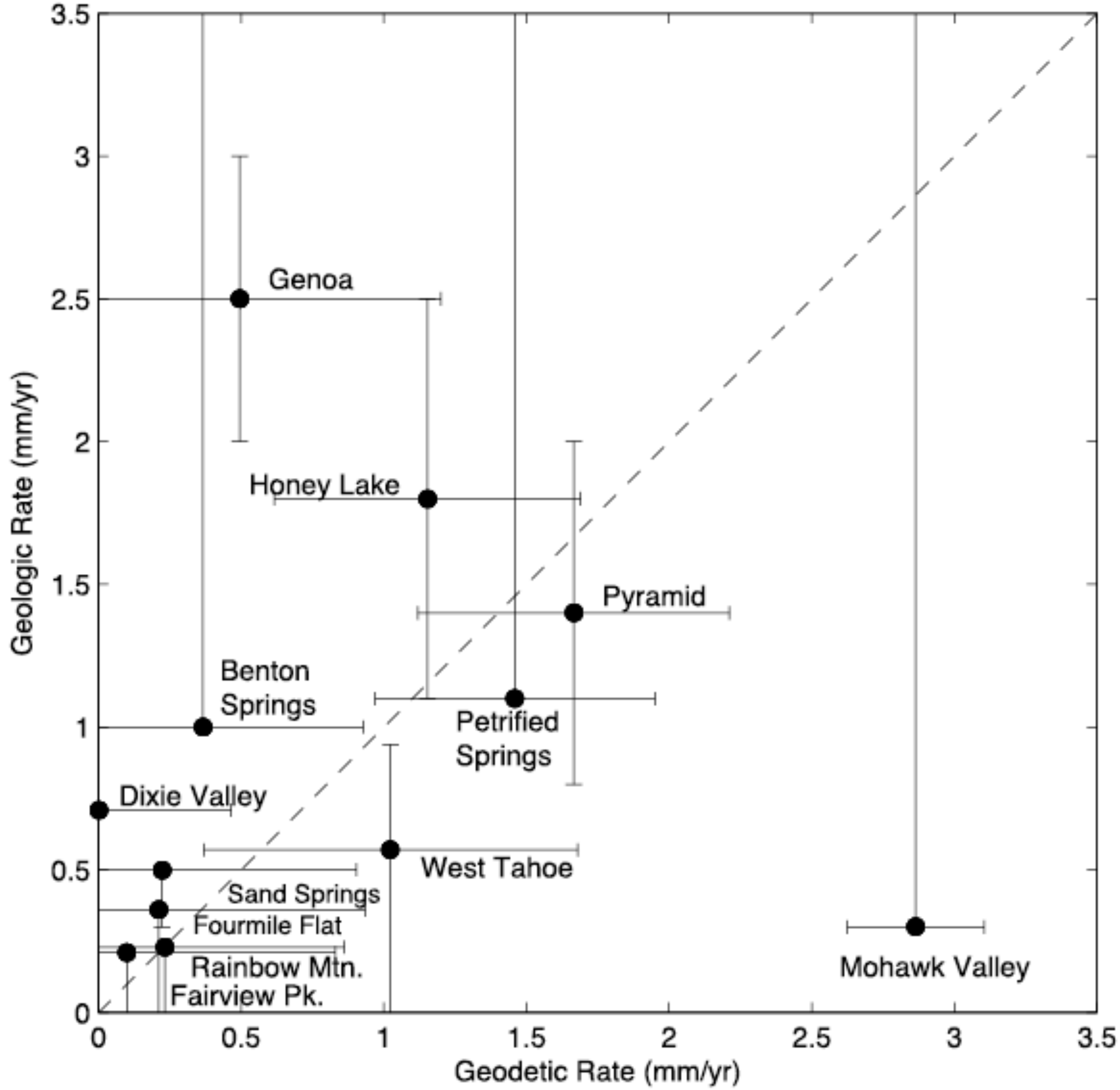

Geologic vs. Geodetic slip rates tend to agree (but not always) and sometimes uncertainties are large....

Figure 14. Comparison between geologic slip rates and slip rates obtained in model shown in Figure 10. Diagonal dashed line indicates where geologic and geodetic slip rates are equal. Names of faults are given and error bars are 2 σ for geologic rates, and sometimes one sided for geodetic rates. See text for discussion.

(from Hammond et al., 2011)

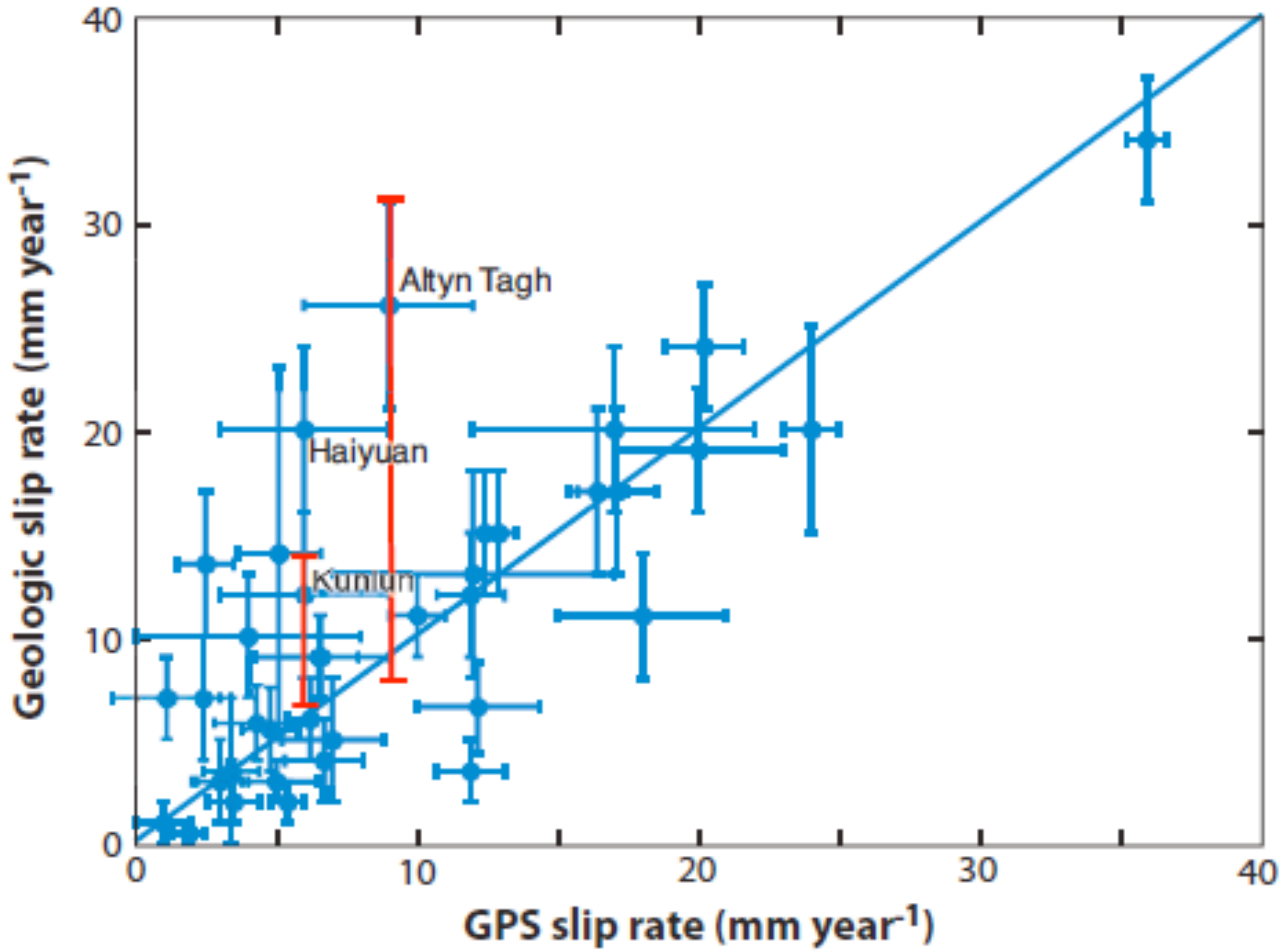

Figure 8

GPS versus geologic slip rates, with 1 SD (standard deviation) error bars, as assigned by each investigator. Determinations for three major strike-slip faults in Tibet are labeled as shown (see **Figure 4** for locations). Red error bars for Altyn Tagh and Kunlun Faults show the larger uncertainty in geologic slip rate estimated by Cowgill (2007). All plotted values are listed in **Supplementary Table 3**.

Thatcher, 2009

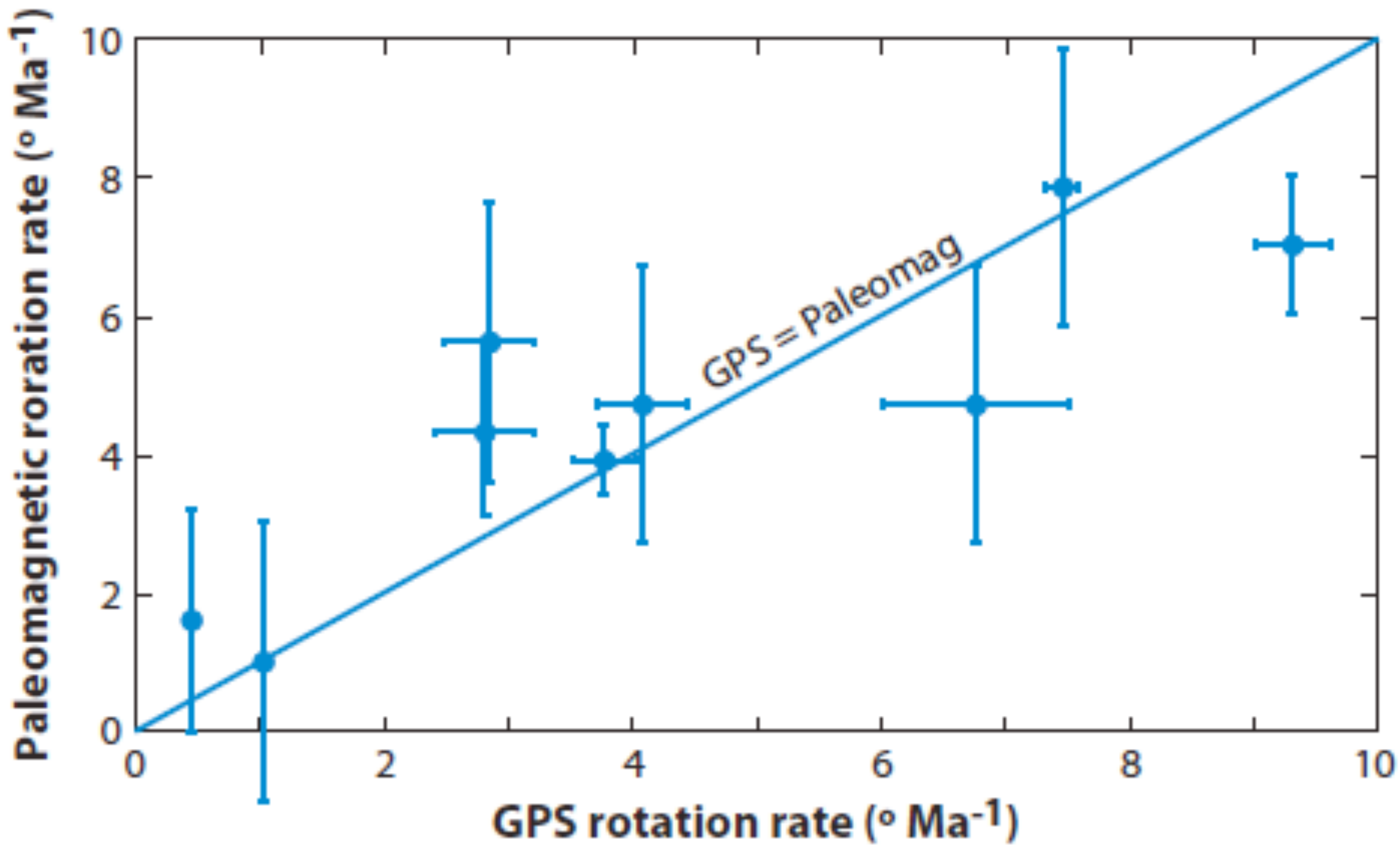

Figure 7

GPS versus paleomagnetic block rotation rates, with 1 SD (standard deviation) error bars as assigned by each investigator.

Thatcher, 2009

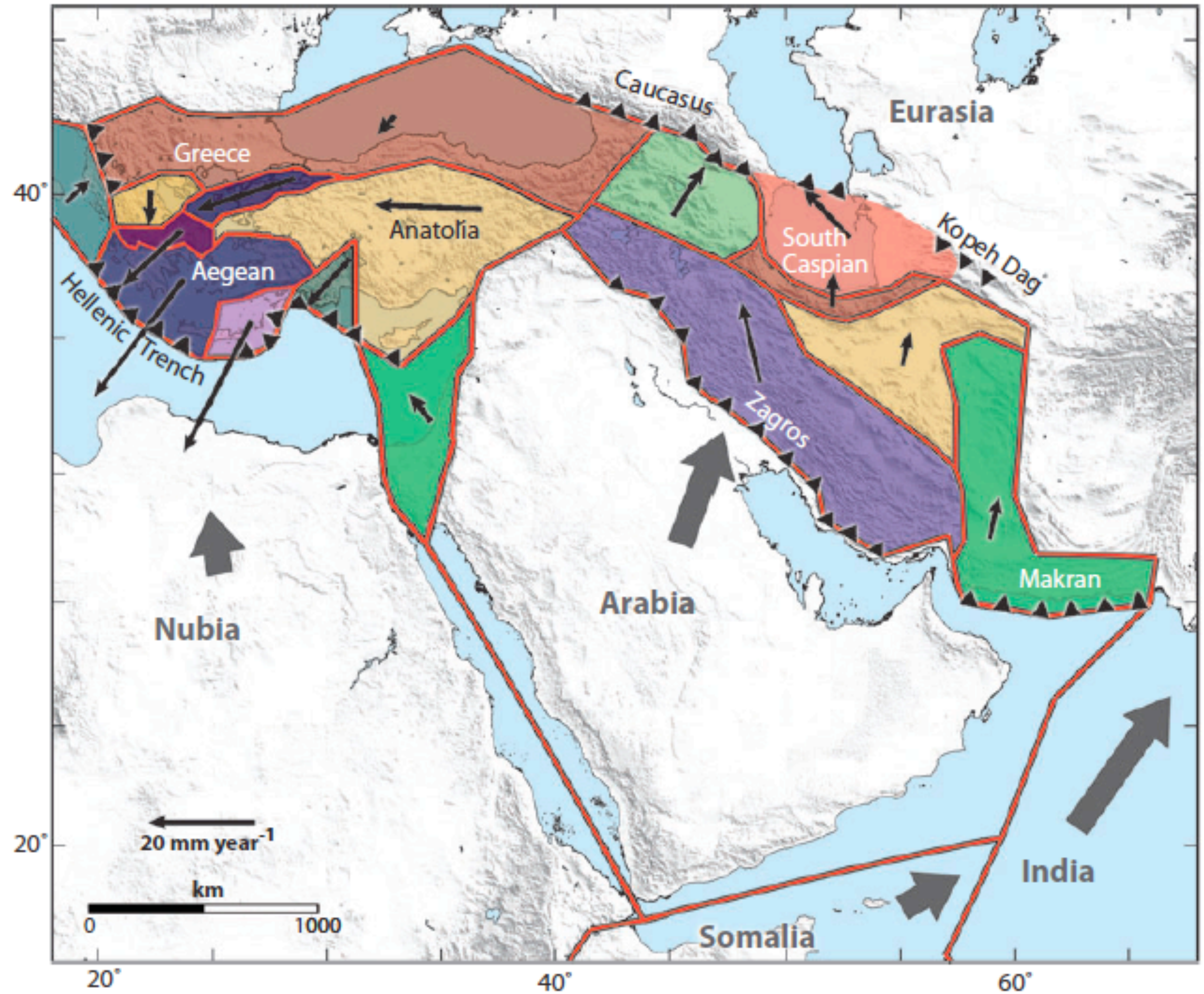

Figure 6

Major global plates (*bold type*) and continental blocks (*colored*) of the eastern Mediterranean and the Middle East, modified from Reilinger et al. (2006). Velocities of major plates relative to Eurasia are shown with large gray arrows. Typical velocities of smaller continental blocks, also relative to Eurasia, have thin black arrows. Solid triangles denote overthrust block at convergent boundaries.

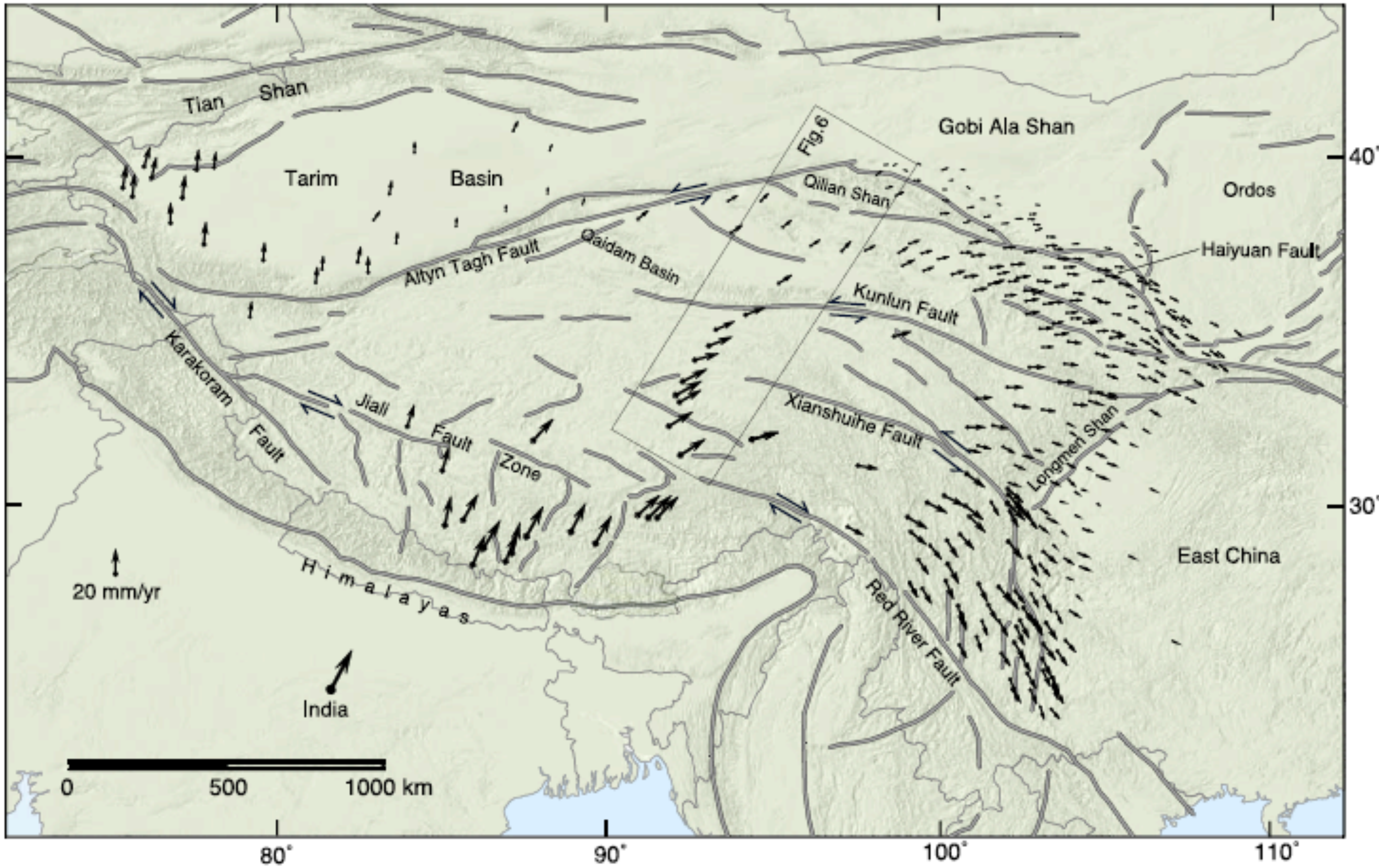

Figure 2. Tibet and surrounding regions, with GPS velocity vectors relative to stable Eurasia (to the north of map area). Velocity uncertainties are generally 1–2 mm/yr, so most error ellipses are illegible at this scale and are not plotted. Gray lines show active faults. Paired arrows show sense of slip on major strike-slip faults (except, to avoid clutter, for the Haiyuan fault, which is left lateral). Major faults and regions discussed in the text are labeled for reference. Rectangle shows location of profile for which observed and model-predicted velocities are plotted in Figure 6.

Thatcher, 2007

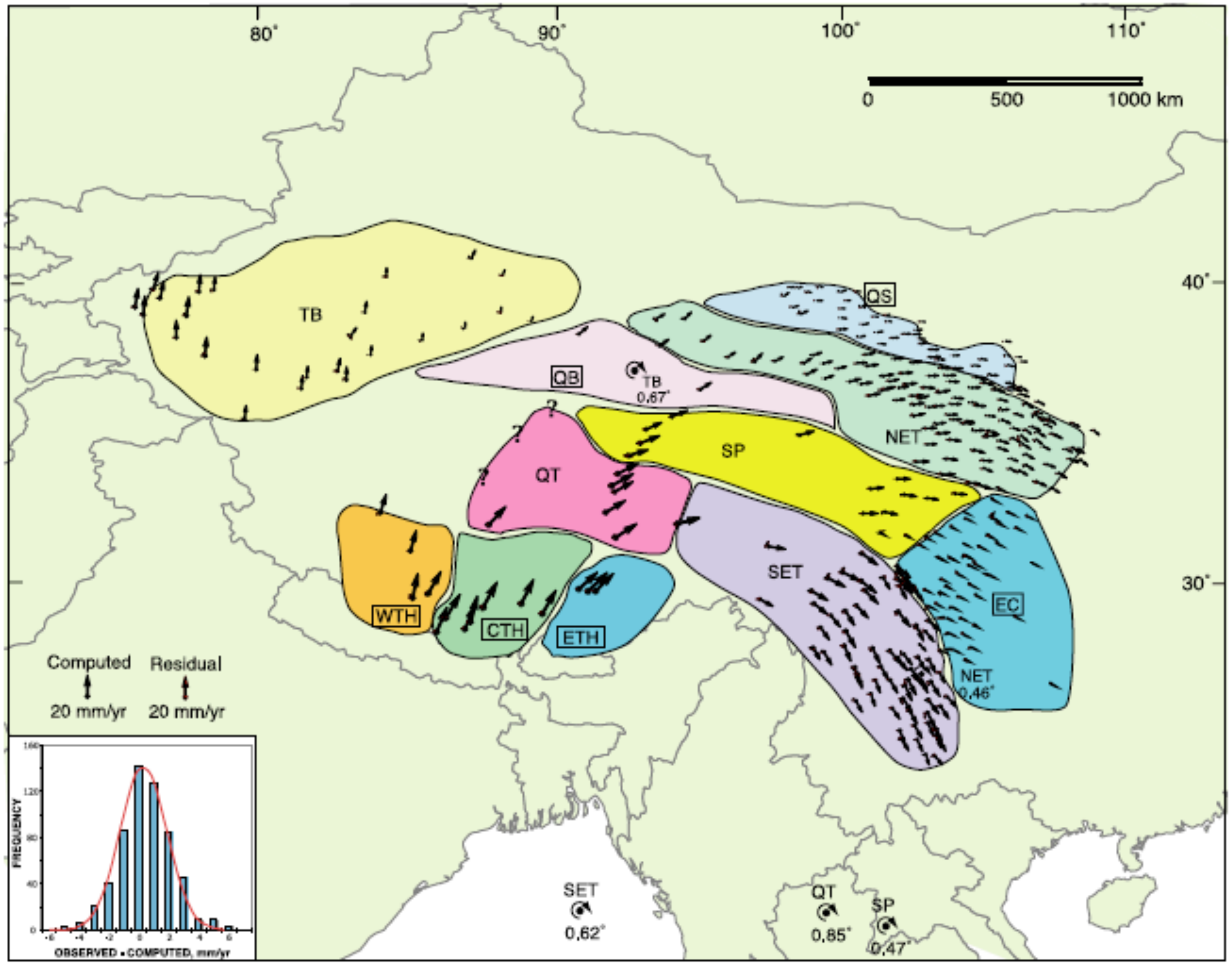

Figure 3. Observed velocity field (black arrows) and block model of Tibet. Blocks are color coded with abbreviated names as indicated. Smaller arrows show differences between observed and computed velocities (many are too small to be seen at true scale; these residuals are shown alone at an expanded scale in Figure 4). Inset shows histogram of residuals, which are fit well by a Gaussian distribution with mean of 0.4 and standard deviation of 1.6 mm/yr. Euler poles (rotation axes) and rotation rates (in degrees per million years) are shown for five blocks (NET, northeast Tibet; QT, Qiangtang; SET, southeast Tibet; SP, Songpan; TB, Tarim Basin). Average translation velocities relative to Eurasia are shown for six additional blocks whose abbreviated names are enclosed by rectangles (CTH, central Tibet Himalaya; EC, east China; ETH, eastern Tibet Himalaya; WTH, western Tibet Himalaya; QB, Qaidam Basin; QS, Qilian Shan). Block model parameters along with data and model fit statistics are listed in Tables 1 and 2.

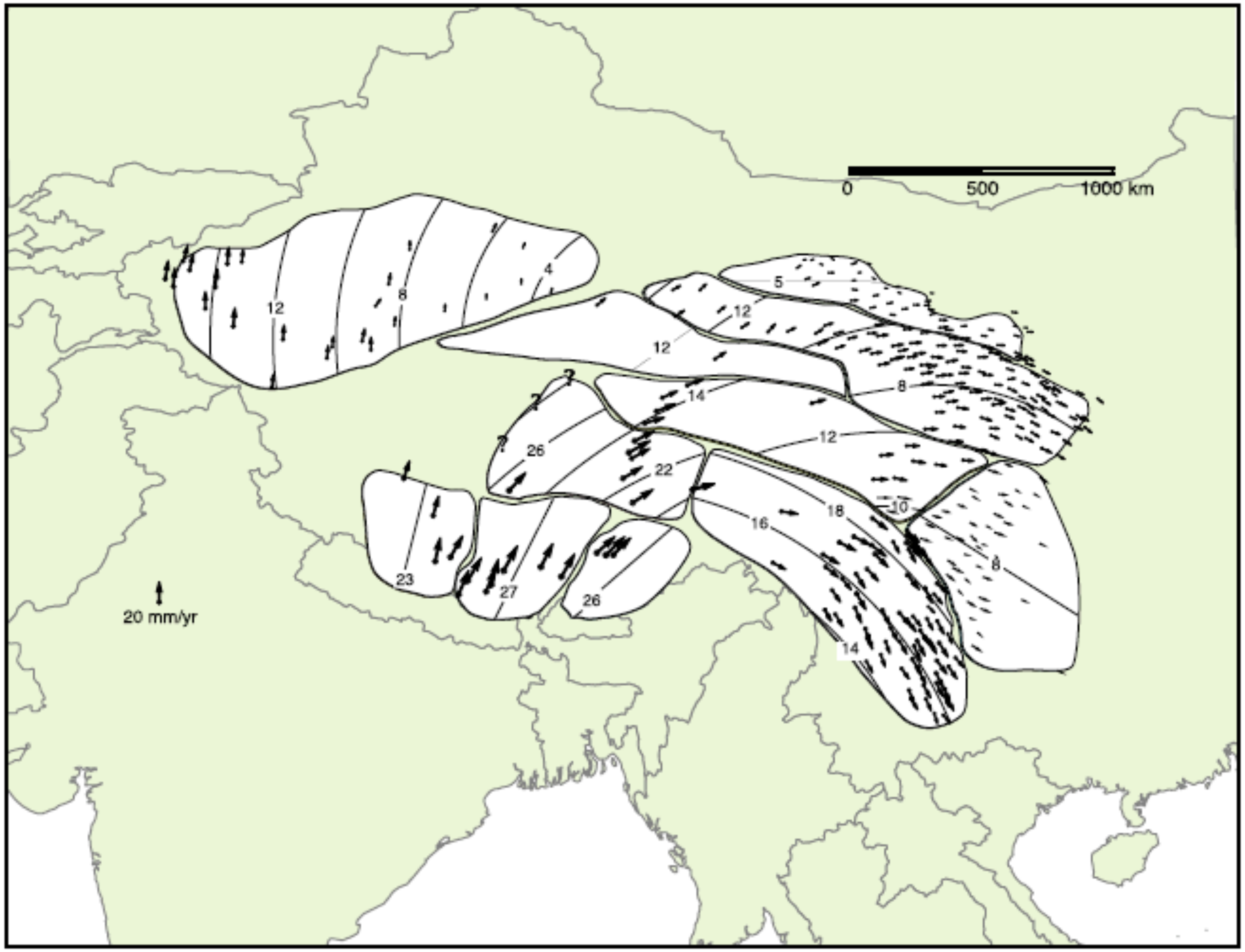

Figure 5. Observed GPS velocities, outlines of blocks used to fit observations, and predicted block motions (faint lines and arcs, with predicted velocities in mm/yr).

Thatcher, 2007

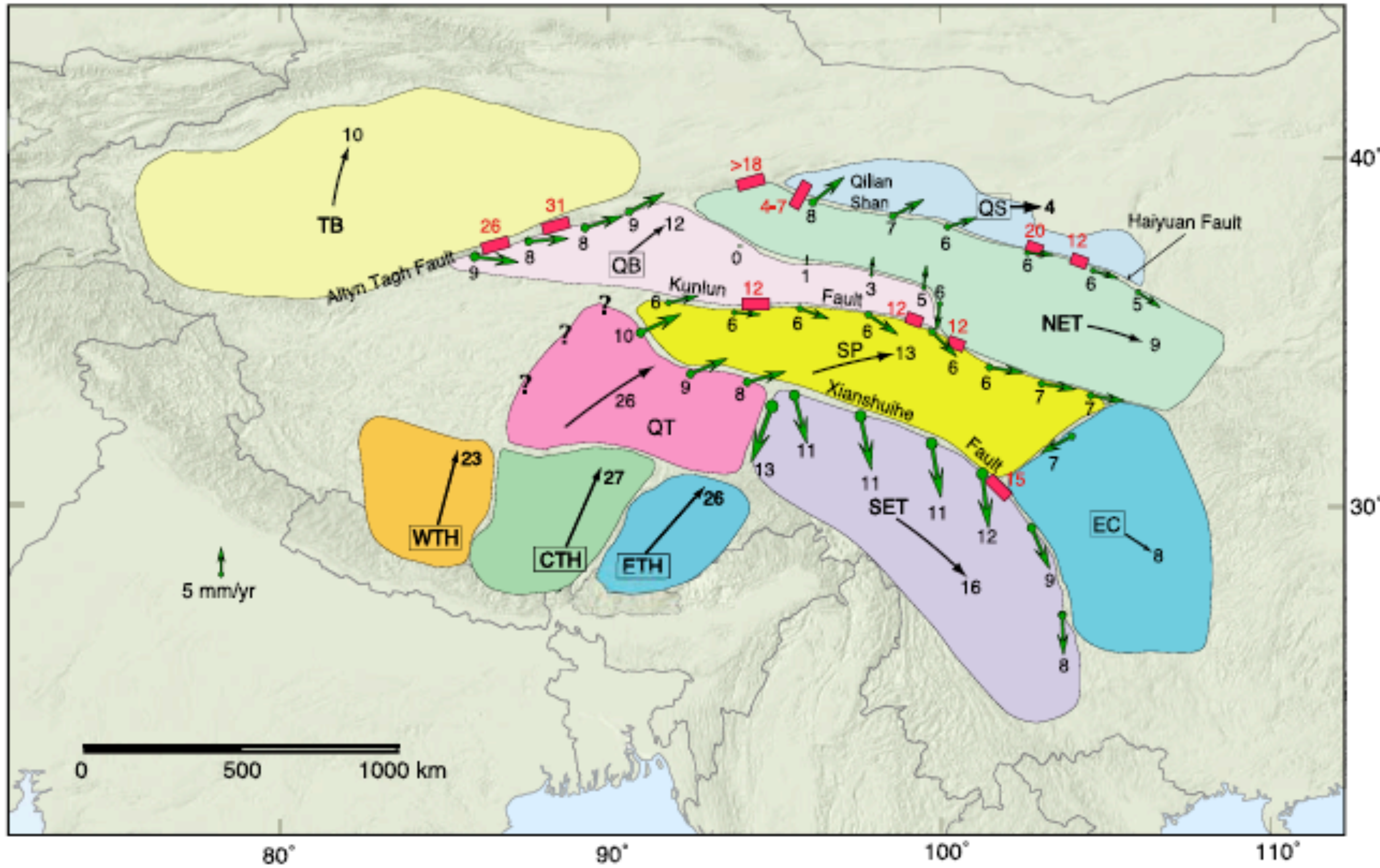

Figure 7. Predicted interblock velocities (thicker green arrows with numbers), with average block velocities relative to Eurasia (thinner black arrows) and geologically estimated slip rates (red numerals). All rates are in mm/yr. Blocks are color coded with names abbreviated as in Figure 3. The convention on interblock vectors is to show the motion of the southern block relative to its northern neighbor, or the eastern block relative to its western mate. Typical rates of motion (relative to Eurasia) near the centers of five rotating blocks are shown by arcs drawn from each of their Euler poles, with arc length proportional to velocity and arrowheads indicating the sense of rotation. The abbreviated names of five additional rigidly translating blocks are enclosed by faint rectangles. Their translation velocities relative to Eurasia are shown as thin straight arrows. Red rectangles show locations of sites where geological estimates of fault slip rate have been obtained by radiometric dating [*Ryerson et al.*, 2006; *Allen et al.*, 1991]; red numerals give the late Pleistocene-Holocene slip rates.

A Thin Viscous Sheet?

(England et al., 1985, 1996)

GEOPHYSICS

The mountains will flow

Philip England

THE key to understanding many geological processes lies in knowing which parts of the solid Earth act as fluids over geological time spans (10^3 to 10^9 years). The fluidity of a system is expressed by its Deborah number, which is the ratio of the length of time needed for flow to occur to the timescale over which a force is applied[1]. The eponymous Deborah prophesied that the mountains would flow before the Lord[2], but contemporary geological opinion is divided on whether mountains flow on a secular basis. On page 37 of this issue[3], Jones *et al.* present evidence that the mountains of western North America, at least, are behaving as a fluid.

Following the success of plate tectonics in describing

Broadly speaking, the aver higher beneath mountain lowlands. We may expect t tains should extend un weight[7] and, more genera ments within continental be from high ground tow This suggestion has quali from the distribution of the eastern Mediterrane the Andes[10], but a quant

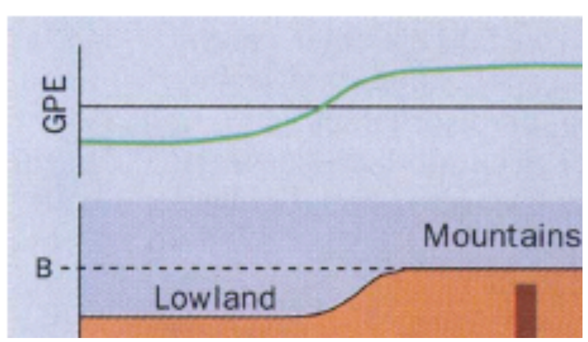

2. SOLUTIONS FOR FLOW IN A SEMI-INFINITE, CONSTANT VISCOSITY, HORIZONTAL LAYER WITH FIXED BOUNDARY VELOCITIES

The force balance for creeping flow is

$$\partial \sigma_{ij}/\partial x_j = \rho g a_i \quad (1)$$

where $a = (0, 0, 1)$, g is the acceleration due to gravity, ρ is density, and σ_{ij} is the (i, j)th component of the stress tensor. The deviatoric stress tensor is

$$\tau_{ij} = \sigma_{ij} + \delta_{ij} p \quad (2)$$

where

$$p = -\tfrac{1}{3}\sigma_{kk} \quad (3)$$

$$\frac{\partial \tau_{xx}}{\partial x} + \frac{\partial \tau_{yx}}{\partial y} + \frac{\partial \tau_{zx}}{\partial z} = \frac{\partial p}{\partial x} \quad (4a)$$

and

$$\frac{\partial \tau_{xy}}{\partial x} + \frac{\partial \tau_{yy}}{\partial y} + \frac{\partial \tau_{zy}}{\partial z} = \frac{\partial p}{\partial y} \quad (4b)$$

For a Newtonian fluid,

$$\tau_{ij} = 2\eta \dot{\varepsilon}_{ij} \quad (5)$$

where η is the viscosity and the strain rate $\dot{\varepsilon}_{ij}$ is defined as

$$\dot{\varepsilon}_{ij} = \frac{1}{2}\left(\frac{\partial u_i}{\partial x_j} + \frac{\partial u_j}{\partial x_i}\right) \quad (6)$$

in terms of the components of the velocity vector $\mathbf{u}$. The velocity satisfies the incompressibility condition

$$\nabla \cdot \mathbf{u} = 0 \quad (7)$$

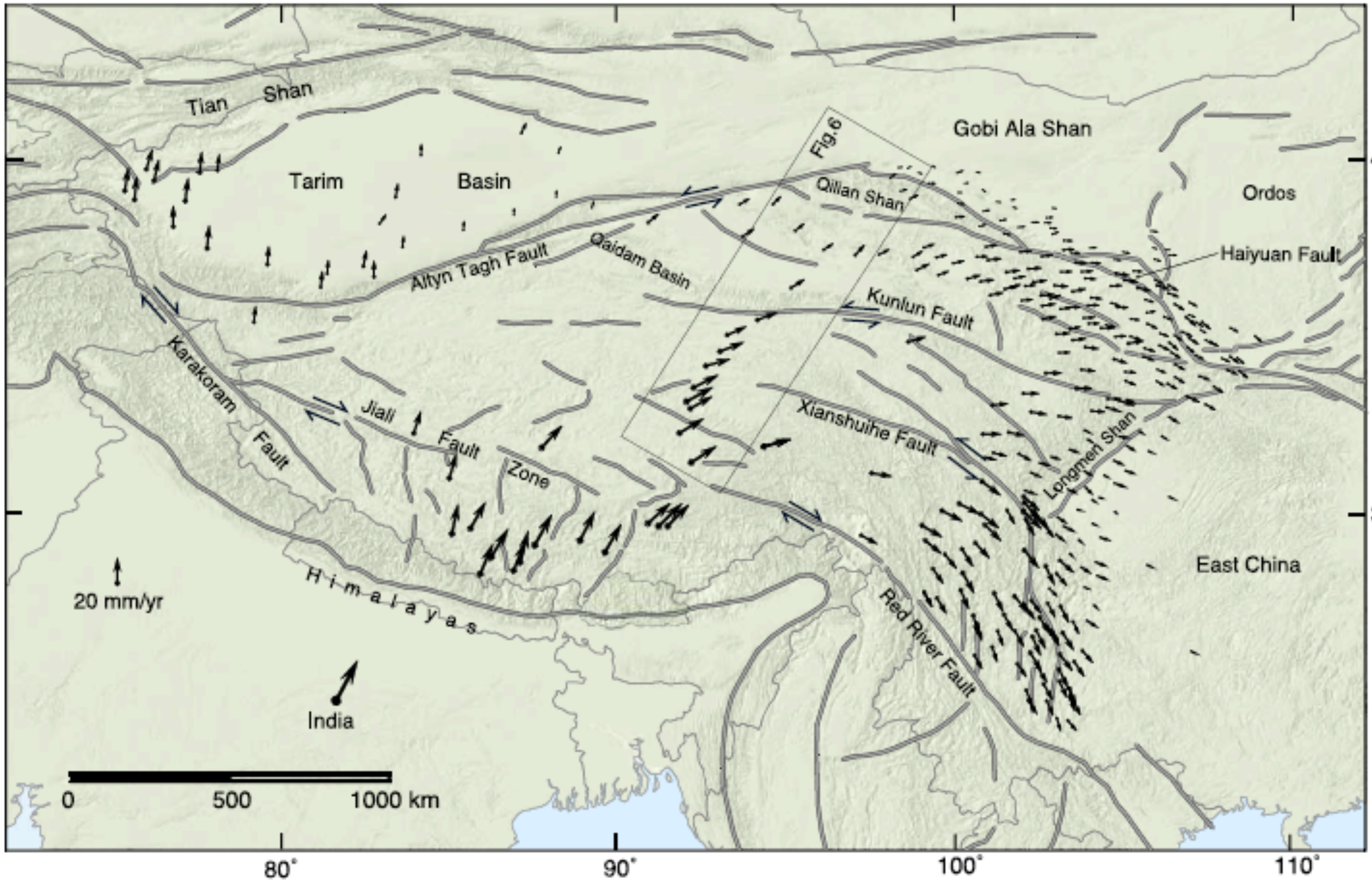

Figure 2. Tibet and surrounding regions, with GPS velocity vectors relative to stable Eurasia (to the north of map area). Velocity uncertainties are generally 1 – 2 mm/yr, so most error ellipses are illegible at this scale and are not plotted. Gray lines show active faults. Paired arrows show sense of slip on major strike-slip faults (except, to avoid clutter, for the Haiyuan fault, which is left lateral). Major faults and regions discussed in the text are labeled for reference. Rectangle shows location of profile for which observed and model-predicted velocities are plotted in Figure 6.

Continuum or Blocky?

Continuum or Blocky?

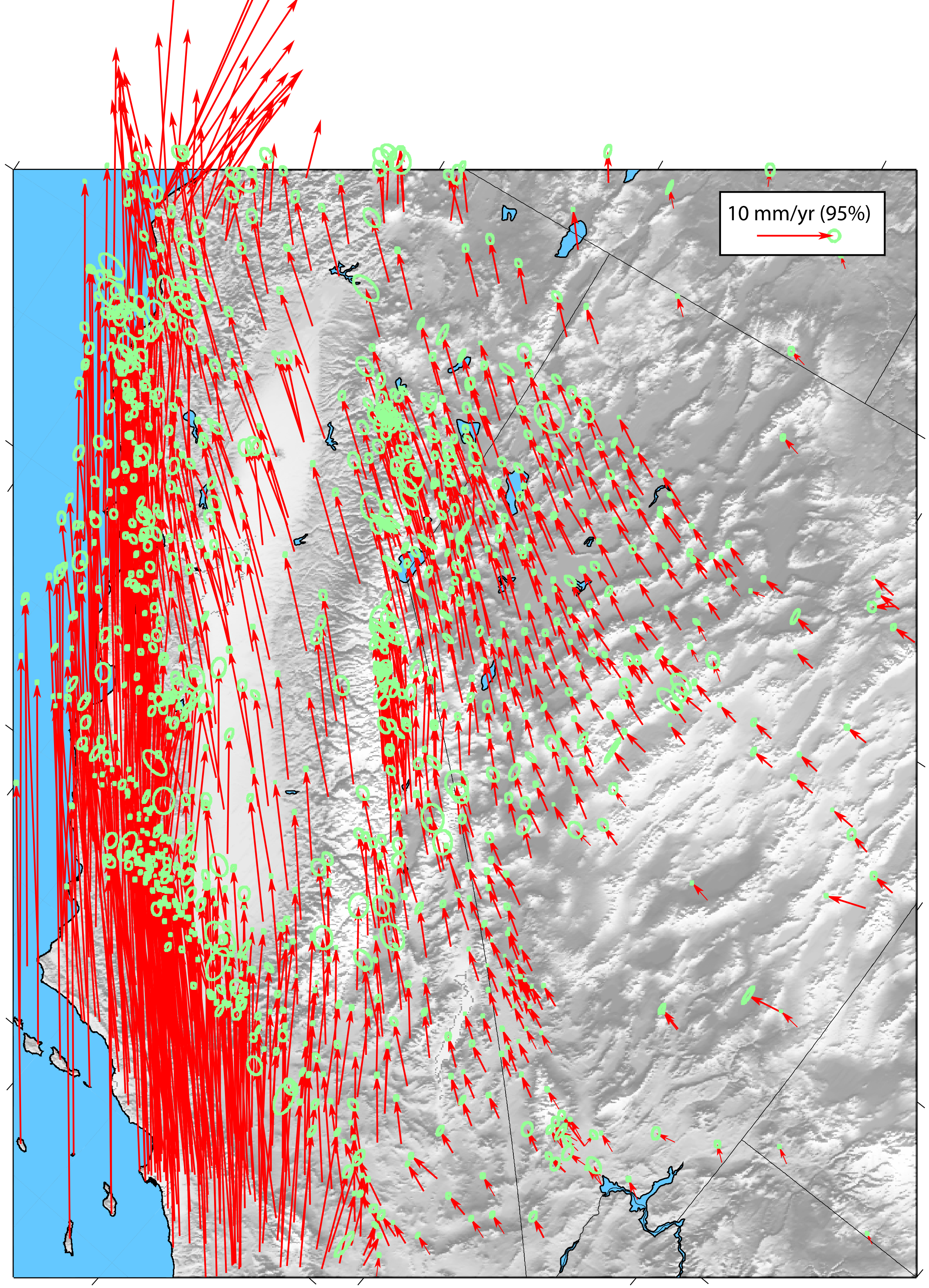

Continuum or Blocky?